University of Twente

The development of single layer hollow fibers based on PES and PVP K90 for outside-in dialysis.

BSc, Biomedical Engineering

N.A. Weening

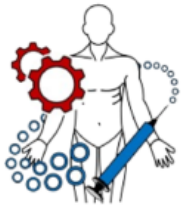

Advanced
Organ bioengineering &
Therapeutics

UNIVERSITY
OF TWENTE.

June 27, 2023

Abstract

English

Chronic kidney disease (CKD) has emerged as a significant contributor to human suffering and mortality in the 21^{st} century. Alarmingly, it stands out as one of the few diseases experiencing an increasing mortality rate in the modern era. With the prevalence of unhealthy lifestyle habits in modern society, it is estimated that there will be a notable rise in the number of individuals affected by chronic kidney disease (CKD). The ideal treatment for these patients would be a kidney transplantation. However, due to limited availability of donor kidneys or compatibility issues, such as blood type mismatch, pose significant challenges. As a result, the majority of patients require alternative therapies to sustain their lives. A therapy often used as kidney replacement is hemodialysis. Hemodialysis makes use of an external filtering device capable of filtering the patients' blood from toxins which would otherwise accumulate within the patient's body. Currently, the patient's blood flows through the fibers that lie within this filtering device, while dialysis solution flows outside of these fibers in the opposite direction. Because of this counter-current flow, the toxins diffuse out of the blood into the dialysis solution through the semi-permeable fiber membrane. The filtered blood is returned to the body. This therapy, however, has multiple downsides. Hemodialysis involves a 3 times per week, 4-hour long session which is not able to remove all toxins from the blood. In addition, the fibers experience blood clotting within the fibers, affecting the filtration capacity. Furthermore, there is a risk of elution of membrane material, specifically polyvinylpyrrolidone (PVP), which can result in structural changes within the membrane. Additionally, the introduction of PVP into the patient's bloodstream may lead to potential health complications. One solution which is currently studied, is the use of outside-in fibers. For outside-in fibers, the dialysis solution flows through the lumen of the fibers, whereas the blood flows through the inter-fiber space, preventing blood clotting of the fibers and increasing the efficiency of the fibers. Multiple outside-in fibers have already been produced and tested with success at the Advanced Organ and bioengineering Therapeutics faculty. Previously, the outside-in fibers were made using a 7 wt.% PVP K90 solution from Sigma-Aldrich. However, with new supplier BASF for the PVP K90, it has been a challenge to successfully fabricate outside-in fibers. It was found that the molecular weight of the new PVP K90 (MW $\approx$ 1000.000 - 1500.000 Da) is significantly higher than the previously used PVP K90 (MW $\approx$ 360.000 Da). To compensate for this increase in molecular weight, outside-in fibers were fabricated using 5.6 wt.%, which did not result in the preferred mechanical and structural properties due to high viscosity of the solution. In this study, a 4 wt.% PVP K90 solution is used to fabricate, characterize and test outside-in fibers using this new PVP K90, comparing them to the previously made 5.6 wt.% PVP K90 (Sigma-Aldrich) fibers and the commercial fibers used for FX high-flux dialyzers of Fresenius. Multiple outside-in fibers were prepared and it has been possible to find methods to directly change the fiber structure and mechanical properties of these new 4 wt.% PVP K90 (BASF) fibers. The fibers with the most promising mechanical properties and structure have been analyzed further by measuring the water permeance and the toxin removal. The water permeance measured was approximately 20 $\pm$ 5 $L\,m^{-2}h^{-1}bar^{-1}$ after a 4000 ppm sodium hypochlorite treatment of 2h. The creatinine removal using spiked plasma (0.1mg/mL) had a value of approximately 1630 $\pm$ 171 after 4h. The dialysanse calculated had a value of approximately 395 $mL\,m^{-2}\,min^{-1}$. The water permeance and the removal of these 4 wt.% PVP K90 fibers were in the range of the commercial FX high-flux dialyzers, as well as the previously made 5.6 wt.% PVP K90 from Sigma-Aldrich fibers. Additionally, this study does give insight in how to manipulate the mechanical and structural properties of these fibers to eventually be able to produce outside-in fibers with excellent toxin removal.

Dutch

Chronische nierziekte (CNZ) is in de 21e eeuw naar voren gekomen als een belangrijke oorzaak van menselijk lijden en sterfte. Alarmerend genoeg is het een van de weinige ziekten die een toenemende sterftecijfer vertoont in het moderne tijdperk. Met de prevalentie van ongezonde levensstijlgewoonten in de moderne samenleving wordt geschat dat het aantal mensen dat wordt getroffen door CNZ aanzienlijk zal toenemen. De ideale behandeling voor deze patiënten zou een niertransplantatie zijn. Echter, als gevolg van beperkte beschikbaarheid van donornieren of problemen met compatibiliteit, zoals onverenigbaarheid van bloedgroepen, brengt dit aanzienlijke uitdagingen met zich mee. Als gevolg hiervan hebben de meeste patiënten alternatieve therapieën nodig om hun leven te kunnen voortzetten. Een veelgebruikte therapie als niervervanging is hemodialyse. Hemodialyse maakt gebruik van een extern filtratiesysteem dat in staat is om het bloed van de patiënt te filteren

van gifstoffen die anders in het lichaam zouden ophopen. Momenteel stroomt het bloed van de patiënt door de vezels die zich binnenin dit filtratiesysteem bevinden, terwijl de dialyseoplossing in tegengestelde richting buiten deze vezels stroomt. Vanwege deze tegenstroom diffunderen de gifstoffen uit het bloed naar de dialyseoplossing door het semi-permeabele membraan van de vezels. Het gefilterde bloed wordt teruggevoerd naar het lichaam. Deze therapie heeft echter meerdere nadelen. Hemodialyse vereist sessies van 4 uur gedurende 3 keer per week, waarbij niet alle gifstoffen uit het bloed kunnen worden verwijderd. Bovendien treedt er bloedstolling op binnenin de vezels, wat de filtratiecapaciteit beïnvloedt. Bovendien bestaat het risico van het vrijkomen van membraanmateriaal, met name polyvinylpyrrolidon (PVP), wat kan leiden tot structurele veranderingen binnen het membraan. Bovendien kan de introductie van PVP in de bloedbaan van de patiënt mogelijke gezondheidscomplicaties veroorzaken. Een oplossing die momenteel wordt bestudeerd, is het gebruik van buiten-naar-binnen vezels. Bij buiten-naar-binnen vezels stroomt de dialyseoplossing door het lumen van de vezels, terwijl het bloed door de tussenvezelruimte stroomt, waardoor bloedstolling van de vezels wordt voorkomen en de efficiëntie van de vezels wordt verhoogd. Meerdere buiten-naar-binnen vezels zijn al met succes geproduceerd en getest bij de faculteit Advanced Organ and Bioengineering Therapeutics. Eerder werden de buiten-naar-binnen vezels gemaakt met een 7 wt.% PVP K90-oplossing van Sigma-Aldrich. Echter, met de nieuwe leverancier BASF voor de PVP K90, is het een uitdaging gebleken om succesvol buiten-naar-binnen vezels te produceren. Er werd vastgesteld dat het molecuulgewicht van de nieuwe PVP K90 (MW $\approx$ 1000.000 - 1500.000 Da) veel hoger is dan de eerder gebruikte PVP K90 (MW $\approx$ 360.000 Da). Om deze toename in molecuulgewicht te compenseren, werden buiten-naar-binnen vezels gefabriceerd met behulp van 5.6 wt.%, wat niet resulteerde in de gewenste mechanische en structurele eigenschappen vanwege de hoge viscositeit van de oplossing. In deze studie wordt een 4 wt.% PVP K90-oplossing gebruikt om buiten-naar-binnen vezels te produceren, karakteriseren en testen met behulp van deze nieuwe PVP K90, waarbij ze worden vergeleken met de eerder gemaakte vezels van 5.6 wt.% PVP K90 en de commerciële fibers die op dit moment gebruikt worden voor de FX dialyse apparaten. Er werden meerdere buiten-naar-binnen vezels gemaakt en het was mogelijk om methoden te vinden om de vezelstructuur en mechanische eigenschappen van deze nieuwe 4 wt.% PVP K90-vezels rechtstreeks te veranderen. De vezels met de meest veelbelovende mechanische eigenschappen en structuur zijn verder geanalyseerd door het meten van de waterdoorlaatbaarheid en het verwijderen van gifstoffen. De gemeten waterdoorlaatbaarheid bedroeg ongeveer 20 $\pm$ 5 $L\,m^{-2}h^{-1}bar^{-1}$ na een behandeling van 2 uur met 4000 ppm natriumhypochloriet. De verwijdering van creatinine met behulp van gespiked plasma (0,1 mg/mL) had een waarde van ongeveer 1630 $\pm$ 171 $mg\,m^{-2}$ na 4h. De berekende dialysance had een waarde van ongeveer 395 $mL\,m^{-2}\,min^{-1}$. De waterdoorlaatbaarheid en de verwijdering van deze 4 wt.% PVP K90-vezels vielen binnen het bereik van de commerciële FX high-flux dialysatoren, evenals de eerder gemaakte 5.6 wt.% PVP K90-vezels van Sigma-Aldrich. Bovendien biedt deze studie inzicht in hoe de mechanische en structurele eigenschappen van deze vezels kunnen worden gemanipuleerd om uiteindelijk buiten-in vezels te produceren met een uitstekende verwijdering van gifstoffen.

Contents

1 Introduction

1.1 Relevance

In the 21^{st} century, Chronic kidney disease (CKD) turned out to be one of the most prominent causes of suffering and death. This progressive condition affects >10% of the general population worldwide, which comes down to >800 million individuals. The leading causes of CKD are diabetes and high blood pressure, often associated with unhealthy habits of the modern way of life such as smoking, drinking too much alcohol, being overweight and too much salt in your diet. These habits are often considered to be a contributing factor to this issue. Kidney failure not only has a significant impact on physical health, but it also takes a toll on mental well-being. Symptoms such as extreme fatigue, nausea, edema, and poor appetite contribute to a decline in physical health. However, the challenges and uncertainties associated with kidney failure can also lead to emotional distress, anxiety, and depression, impairing mental health. The therapy often used to replace kidney function is hemodialysis, an intermittent therapy which involves a 3 times per week, 4-hour long session and has significant consequences on the patient's life. Unfortunately, this therapy does not work optimal since not all toxins are removed from the patients blood. The dialysis device used contains fibers necessary for the filtration of blood, but these fibers experience blood clotting within the fibers, affecting the filtration capacity of the dialysis device. Moreover, elution of membrane material can occur which causes alterations to the membrane's structure and characteristics, and causes material of the membrane fibers to enter the patients blood. Because of these problems, it is necessary to improve this kind of therapy for CKD patients [1].

1.2 The kidney

The kidneys are bean-shaped organs, located just below the rib cage with one on each side of the spine. Kidneys are responsible for removing toxins from the blood and regulation of concentrations of salts and other dissolved substances. The three main types of waste are protein-bound toxins (hippuric acid (HA), indoxyl sulfate (IS)), middle molecules (β_2-microglobulin) and small water-soluble toxins (creatinine, urea). If the kidney fails to maintain the correct balance between the salts and dissolved substances, it affects other parts of the body such as nerves and muscles. The kidneys also produce hormones responsible for controlling blood pressure, making of red blood cells and maintaining healthy bones [2]. Both kidneys are composed of a million nephrons, functioning as filtering units. Each nephron consists a filter, the glomerulus, and a tubule. As blood flows through each nephron, it first enters the glomerulus, a cluster of small blood vessels. Here, the thin walls of the glomerulus allow for the passage of smaller molecules, waste products, and mostly water into the tubule. The larger molecules that can not pass the thin wall such as proteins and blood cells remain inside the blood vessels. Subsequently, the tubule selectively reabsorbs necessary substances such as minerals, nutrients and almost all of the water back into the blood vessels which run alongside it. The tubule also plays a role in removing excess acid from the blood. The remaining fluid and waste products in the tubule eventually form urine. The schematic representation of the kidney function is displayed in figure 1 [2][3].

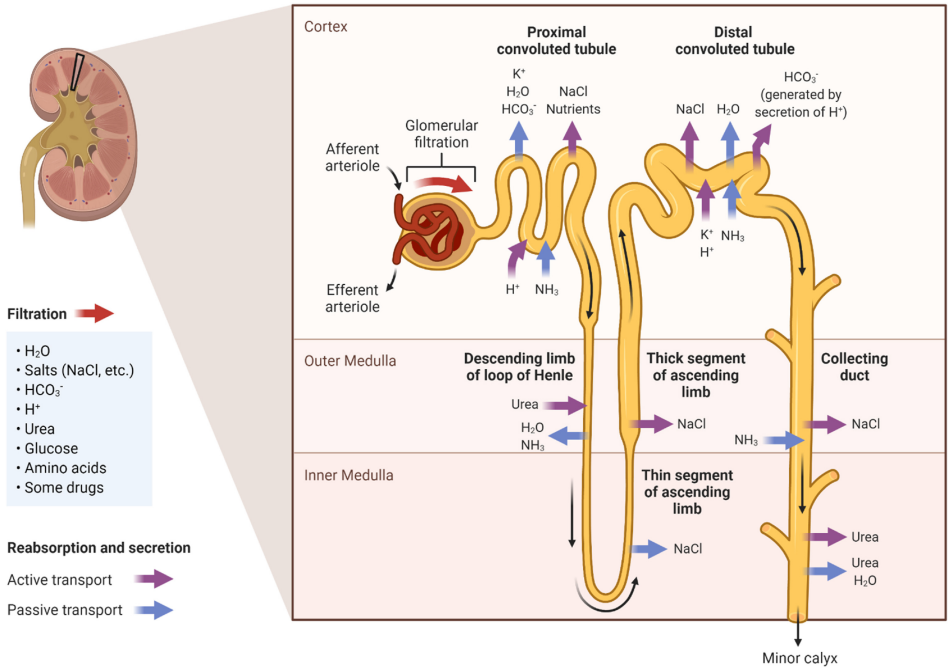

Figure 1: Schematic representation of the kidney function [2].

1.3 Kidney failure

The main causes for kidney failure are high blood pressure and diabetes. Patients with diabetes have a high blood sugar level which can damage the kidney blood vessels and nephrons, resulting in a lower filtration ability of the kidneys. High blood pressure means your body pumps blood faster through the blood vessels as normal. This can cause damage to the blood vessels, such as the kidney blood vessels. This damage leads to less blood flowing to the kidneys and therefore limiting the kidneys filtration function. When the kidneys lose the ability of filtering the waste from the blood, excess fluid and waste from the blood accumulate in the body which could potentially cause other health problems, such as a stroke or heart disease. If the abnormality in the kidney structure or functions lasts more than 3 months, it is called a chronic kidney disease (CKD). This progressive condition affects >10% of the general population worldwide, which comes down to >800 million individuals. Unlike other kidney diseases, such as acute kidney disease (AKD), CKD is irreversible and therefore no after treatment recovery is possible. CKD can be classified in different stages, ranging from G1 to G5. The stages are based on the glomerular filtration rate (GFR)(mL/min/1.73m^2). To determine the patient's state, a blood test can be performed to measure the creatinine level of the patient's blood. This amount, together with extra patient information, is used to determine the estimated glomerular filtration rate (eGFR). Individuals with an eGFR of less than 60mL/min/1.73m^2 measured twice, 90 days apart, is said to have CKD. Besides the GFR categories, another categorie is used for the classification of CKD, the albumin: creatinine ratio (ACR). This is measured by performing an urine test and, as expected, measures the ratio between albumin and creatinine in the urine. As shown in figure 2, the ACR has 3 stages. By combining both GFR and ACR, the final classification of CKD is determined ranging from G1A1, indicating a healthy kidney, to G5A3 where G5 is often called the end-stage renal disease (ESRD), see figure 2 [4][5].

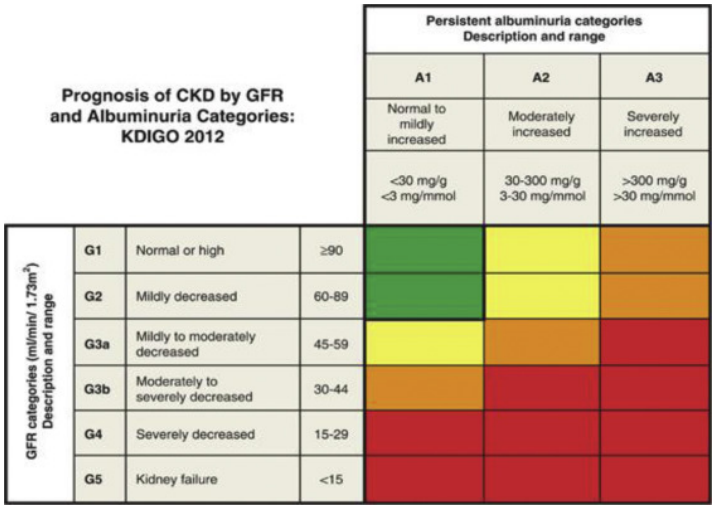

Figure 2: Classification of CKD stages based on GFR and ACR [4].

It is no question that the kidneys will get worse over time, but it is possible to slow this process down by giving a strict diet and multiple kinds of therapies to the patient. If no therapy or diet is used, the CKD could become AKD and potentially be lethal. Therefore, it is important that CKD patients receive the right therapy [4].

1.4 Therapies

1.4.1 Dialysis

The best treatment would be a kidney transplantation. However, due to limited availability of donor kidneys or not having the same blood type as the donor, most patients need alternative therapies to stay alive. One therapy that is often used to compensate for the lack of removal of waste and extra water from blood is called dialysis, an artificial replacement of the most important function of the kidney. If the patient is in stage 5, $<$ 15 mL/min/1,73 m^2, dialysis is performed to remove accumulated toxins from the body. The basic principle of dialysis involves the diffusion of toxins across a semipermeable membrane with help of dialysis solution containing pure water, electrolytes and salts. The substances considered as metabolic waste products within the blood, such as creatinine and urea, diffuse from the bloodstream into the dialysis solution following the concentration gradient. The diffusion rate of these solutes across the membrane is influenced by the size of the particles, with larger particles exhibiting a slower rate of diffusion than smaller ones [6]. The dialysis can be divided into two types; hemodialysis where an artificial kidney-like machine is used or peritoneal dialysis where a patient's own peritoneal membrane is used as filter, see figure 3.

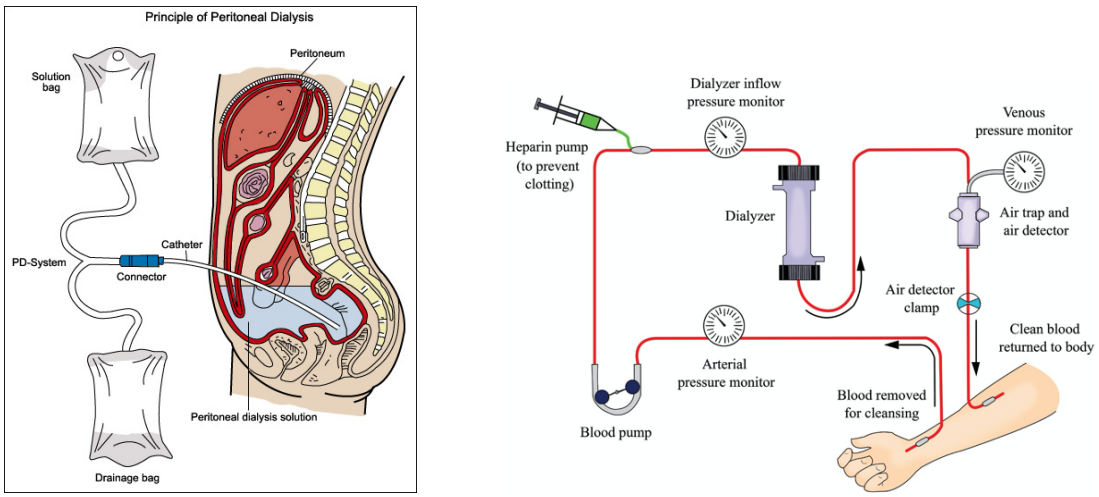

(a) Process of peritoneal dialysis [7].

(b) Process of hemodialysis [8].

Figure 3: The difference between the peritoneal dialysis and the hemodialysis.

For peritoneal dialysis, the blood filtering happens within the body by using the peritoneal lining as filter. Dialysis solution moves through a catheter into the abdomen untill the bag is empty. The dialysis solution absorbs extra fluid and wastes from the body and is drained out of the abdomen after a few hours. Only a minor operation is needed to perform this procedure. This procedure can easily be done at home and does not need big machines. Although this sounds deceiving, there are a few disadvantages with peritoneal dialysis. For instance, there is an increased change of developing infections inside the abdomen, called peritonitis. It should also be considered that peritoneal dialysis needs to be performed every day. There will also be a catheter, a thin tube, left in the abdomen permanently. Figure 3a shows schematically the working of peritoneal dialysis.

In contrast to peritoneal dialysis, hemodialysis uses an external device containing a semipermeable membrane, dialyzer, to filter the patients' blood. Here, blood leaves the body into the dialyzer where a counter-current flow is present, with blood flowing in one direction and the dialysis solution in opposite direction. Because of the counter-current flow, the waste products diffuse out of the blood into dialysis solution and filtered blood is returned to the body. Figure 3b shows schematically the working of hemodialysis. The flexibility of the peritoneal dialysis and the ability to do it at home could make this type more desirable, especially for younger, active people. For patients with no remaining kidney function, hemodialysis is used [6].

This study will focus on hemodialyses, which is the most common type of dialysis used. Unfortunately, this dialysis process is time-consuming and significantly affects the patient's quality of life. The dialysis is a 4 hour process 3 times a week which not only has inadequate removal of waste solutes and excess water, but also effects the well being of the patient. To improve the quality of life for these patients', the ultimate goal is identifying long-term and/or continuous therapies that can effectively eliminate toxins from the blood plasma. To achieve this, one requires dialyzers containing hollow fibers with prolonged blood compatibility and exceptional resistance to fouling.

1.4.2 Principe of hollow fibers

The hollow fibers currently used for dialysis consist of a selective inner layer and a fiber wall which is assuring stability of the fiber, which could be both with macrovoids or a sponge-like structure. Figure 4 displayes the difference between a sponge-like structured wall and a macrovoid-structured wall.

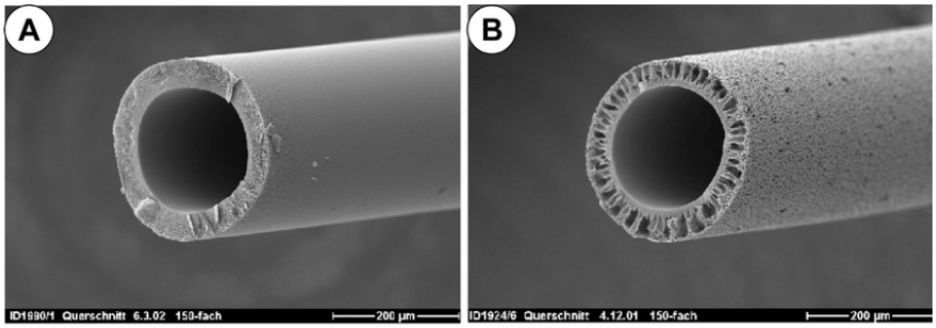

Figure 4: Difference between a sponge-like structured wall (A) and a macrovoid-structured wall (B) [9].

Currently, blood flows through the lumen of these hollow fibers, while dialysis solution circulates through the interstitial space of the fibers. This filtration modus is called inside-out filtration. The selective inner layer of the hollow fiber is responsible for the diffusivity of the toxins present in the patients' blood.

Furthermore, the selective layer acts as a safeguard, ensuring the preservation of red blood cells, white blood cells, and platelets within the bloodstream. Its precisely defined cut-off restricts the passage of these vital components, effectively shielding them from filtration. By exploiting the concentration gradient generated by the counter-current flow between the blood and dialysis fluid, toxins such as creatinine permeate through this selective inner layer. Subsequently, the toxins travel through the fiber walls and end up in the dialysis solution.

1.4.3 Components

To create the inside-out hollow fibers consisting of a selective inner layer, a porous outer layer, and the fiber wall, a combination of solvent, non-solvent and one or more polymers is required. Since this study uses multiple polymers, this will be discussed further. The solvent plays a huge role in dissolving the polymers. A solvent often used is N-Methyl-2-pyrrolidone (NMP), which will also be used as solvent during this study. Distilled water serves as the non-solvent in this study. As for the polymers, a blend of hydrophobic and hydrophilic polymers is typically employed. In this case, the hydrophobic polyethersulfone (PES) polymer and the hydrophylic polivinylpyrrolidone (PVP) polymer are used.

Polyethersulfone (PES) PES is widely used in the biomedical fields such as artificial organs and hemodialysis due to its thermal and hydrolytic stability, excellent mechanical properties, and high permeability for low-molecular-weight proteins when employed in hemodialysis membranes. However, because of the hydrophobic properties of PES, the blood proteins are rapidly absorbed by the PES membrane which can result in particle aggregation or platelet adhesion on the membrane's surface. This hydrophobic particle absorption causes membrane fouling, limiting the membrane's lifespan and filtration performance. Therefore, the hollow fiber membranes are often modified using a hydrophilic polymer, as is the case with PVP in this study [10].

Polivinylpyrrolidone (PVP) The hydrohilic properties of PVP enhance the overall hydrophilic properties of the membrane, improving its blood compatibility of the membrane and therefore decreasing the absorption of hydrophobic particles onto the membrane, limiting membrane fouling. Additionally, PVP also serves as a pore-forming agent and contributes to the creation of the selective layer [10].

1.4.4 Formation of fiber membrane

To form the inside-out fibers, PES and PVP are dissolved in the solvent NMP, forming the dope solution. This dope solution is extruded through a so-called spinneret, to form hollow fiber membranes. Additionally, there is a bore solution, a coagulation bath and an airgap. For the inside-out fibers (IOF), which feature a selective inner layer and a porous outer layer, the bore solution consists of ultrapure water and the coagulation bath of distilled water.

The bore solution flows through the center of the spinneret, while the dope solution surrounds it, see figure 5. The use of a bore solution ensures that a lumen is formed and a hollow fiber is created.

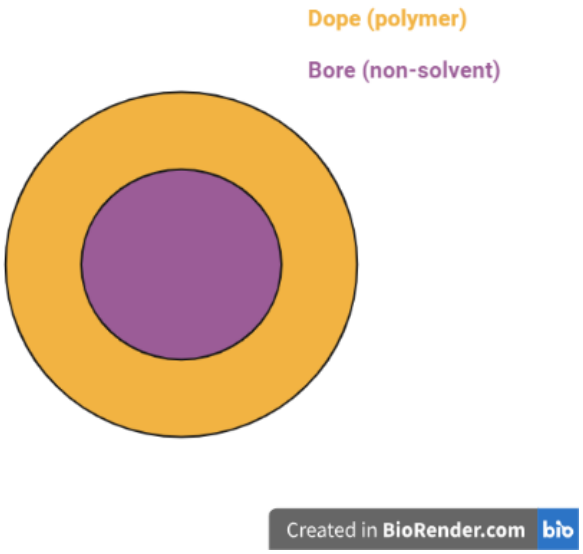

Figure 5: Schematic representation of the solutions within the spinneret for fabricating inside-out fibers.

Because of the hydrophilic properties of PVP, PVP is attracted to the ultrapure water present in the bore solution. As the bore solution contains 100% water, the hydrophilic PVP migrates towards the bore solution, resulting in a higher concentration of PVP on the inside of the fiber compared to the outside. Moreover, a fast exchange between NMP of the dope solution and water of the bore solution, results in the formation of the selective layer. Once the solution exits the spinneret, an air-gap is present before it enters the coagulation bath. The air gap is responsible for the following:

A relatively large air gap between the spinneret and the surface of the coagulation bath, delays the phase separation of the polymer solution and results in the formation of relatively larger pores on the fiber outer walls, when compared to a relatively small air gap. Since the amount of water present in the air is different from the amount present in the coagulation bath, the fibers' morphology can be "tuned" by varying the air gap.

The NMP present in the dope solution undergoes an exchange with the water present in the coagulation bath. As a result, NMP present in the solutions diffuses into the coagulation bath, while water present in the coagulation bath infiltrates the dope solution, turning the liquid solution into a solid fiber. Not only is the water within the coagulation bath attracted to the NMP, but also to the hydrophilic PVP present within the dope solution. The PVP will therefore lay around the water which is present between the polymers. This movement of PVP towards the water leads to the formation of a porous structure. The swiftness of the exchange between NMP and water determines the size of the formed pores, with faster exchange resulting in smaller pores. In addition, the more PVP is present, the more water is surrounded by the PVP and thus again the smaller the pores are formed. When a lot of small pores are formed, a sponge-like structure can be observed.

1.5 Previous studies

1.5.1 Clotting of dialyzers

Currently, the blood flows through the lumen of the fibers while dialysis fluid flows in the inter-fiber space, using inside-out fibers (IOF). However, fiber clogging occurs due to thrombus deposition in the fiber lumens caused by the blood, limiting filter life to approximately 15-40h and results in less open fibers and therefore less effective membrane surface area to filtrate the patients' blood [11]. Based on the oxygenerators, outside-in fiber (OIF) modus for dialysis was studied and tested. Instead of blood flowing through the fibers, the blood is present in the inter-space of the fibers and dialysis fluid will flow through the lumen of the fibers. Therefore, the new fibers should have a thin-selective layer at

the outside of the fiber instead at the inside of the fiber like the commercial fibers, displayed in figure 6.

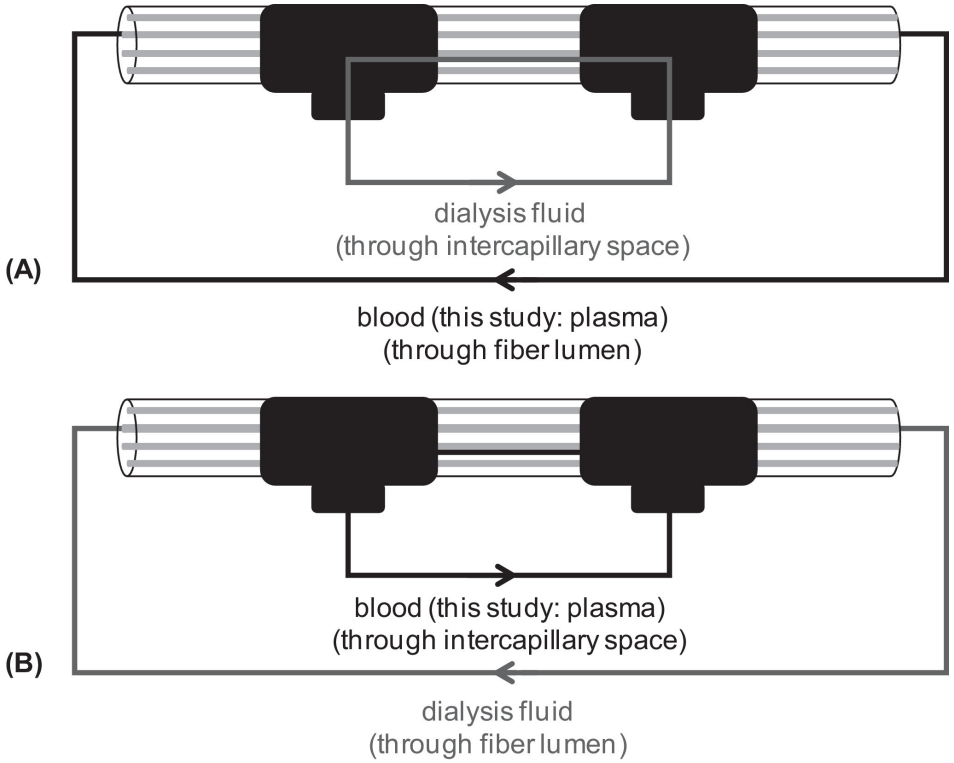

Figure 6: Illustration of flow directions of blood and dialysis fluid [12].

Duhkin et al studied the difference between OIF and IOF fibers, specifically focused on the effect of clotting and duration of the fibers [11]. They showed that the commercial fibers can last up to 100h with the OIF mode. Furthermore, it was observed that there was a reduced occurrence of blood clotting, which was limited to the exterior of the fiber bundle near the blood entrance of the dialyzer. This phenomenon resulted in a higher maintenance of the effective membrane surface area. In addition, thrombus formation was observed to occur in the inter-fiber space rather than within the fiber lumens, which had a small impact on the axial pressure drop as blood was able to bypass the blockage. Figure 7 and 8 show the difference in clotting for the IOF and OIF mode.

Figure 7: Clotting resulting from the inside-out filtration mode [11].

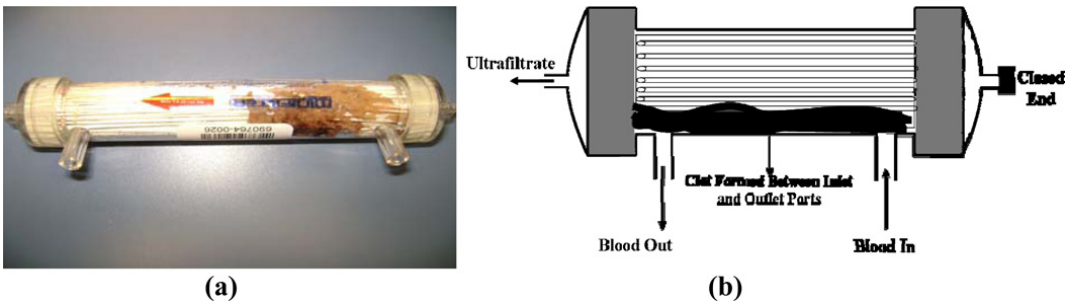

Figure 8: Clotting resulting from the outside-in filtration mode [11]

These studies thereby prove that outside-in fiber modus improves the efficiency of the dialysis process. Since the blood will be present at the outside of the fibers, while the dialysis solution will be inside the fibers, new fibers suited for this new situation are needed. Therefore, outside-in composition fibers need to be made with a thin selective layer on the outside of the fiber and a porous inner layer[11][13].

1.5.2 Elution of PVP

Not only is there thrombus formation within the fibers, the hydrophilic polymer PVP could leach out from the membranes during long-term dialysis which could potentially cause health issues for the patient and lead to membrane fouling. As mentioned before, PVP is responsible the hydrophilic properties of the fiber membrane, preventing absorption of hydrophobic particles which could cause membrane fouling. Moreover, elution of PVP also causes formation of bigger pores, resulting in a less-selective layer. Therefore, today's dialyzers are not suited for long-term dialysis and a new dialysis filter is needed to achieve the goal of long-term dialysis, prevent blood clotting and membrane fouling and improve the patients' quality of life [13].

1.6 This study

In order to fabricate outside-in fibers, the bore solution will consist of a mixture of NMP and ultrapure water to slow down the exchange between water and NMP and thus form bigger pores on the inner layer. As for the outer layer of the fiber, it is preferred to directly drop the fiber inside the coagulation bath to have a fast exchange between the water and NMP and form the selective outer layer. Because this is not possible, a shower solution is used consisting of 100% ultrapure water, see figure 9. This, in combination with the PVP moving now more to the outside of the fibers, will create a more hydrophilic outside of the fibers, with smaller pores and a sponge-like selective layer.

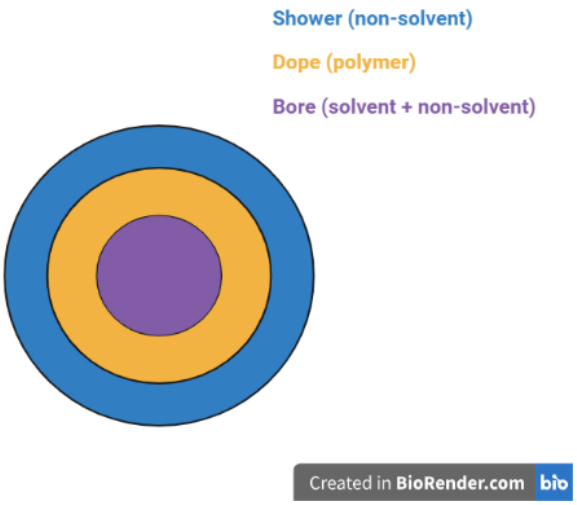

Figure 9: Schematic representation of the solutions within the spinneret for fabricating outside-in fibers.

Within the Advanced Organ Bioengineering and Therapeutics group, these high flux outside-in fibers have already been prepared and tested multiple times using polivinylpyrrolidone (PVP) as the hydrophilic additive and polyethersulfone (PES) as the hydrophobic polymer. However, a recent challenge has emerged due to the adoption of a new supplier of the PVP component. This resulted in a significant alteration in the fibers' mechanical properties compared to the previously used PVP. As a consequence, the process of producing fibers with consistent mechanical properties started again. Normally, the production of these fibers involved utilizing a 7 wt.% PVP K90 from Sigma-Aldrich solution. However, with the introduction of the new supplier, BASF, it has become increasingly challenging to achieve the desired results using this particular concentration. The main difference between both suppliers is the molecular weight of the PVP K90 polymer. The molecular weight of the PVP K90 from BASF (MW $\approx$ 1000.000 - 1500.000 Da) is higher than the molecular weight of the PVP K90 from Sigma-Aldrich (MW $\approx$ 360.000 Da), making it challenging to achieve the desired results using the old settings and solutions. Multiple testing has been done using different concentrations of PVP K90 from BASF, with a focus on a 5.6 wt.% PVP K90, 12 wt.% PES and 82.4 wt.% NMP dope solution. Below, the results of the best produced OIF-PVP5.6 fibers are represented, all made using the same dope solution as mentioned before. Table 1 shows the spinning conditions used for the OIF-PVP5.6 hollow fibers, figure 10 shows the SEM images and table 2 the measurements for these fibers as well as the preferred dimensions based on the commercial fibers. For the OIF-PVP5.6 hollow fibers, the pulling wheel speed and the bore solution were varied. The rest of the parameters and solutions were kept the same. For the OIF-PVP5.6-1 hollow fibers, a pulling wheel speed of 9.0 m/min and a bore solution of 75/25 NMP/ultrapure water was used. For the OIF-PVP5.6-8 hollow fibers, the pulling wheel speed was changed to 4.5 m/min whereas. For the OIF-PVP5.6-11 hollow fibers, the pulling wheel speed of OIF-PVP5.6-8 was kept the same, but the bore solution was changed to a 50/50% NMP/ultrapure water solution.

Table 1: Spinning conditions for the OIF-PVP5.6 fibers.

Parameters	**OIF-PVP5.6-1**	**OIF-PVP5.6-8**	**OIF-PVP5.6-11**
Dope pumping speed ($mL\,min^{-1}$)	1.0	1.0	1.0
Bore liquid pumping speed ($mL\,min^{-1}$)	0.4	0.4	0.4
Shower pumping speed ($mL\,min^{-1}$)	0.4	0.4	0.4
Air gap (cm)	1.2	1.2	1.2
Pulling wheel speed ($m\,min^{-1}$)	9.0	4.5	4.5
Bore solution (NMP/MilliQ)	75/25%	75/25%	50/50%
Shower solution	100% MilliQ	100% MilliQ	100% MilliQ

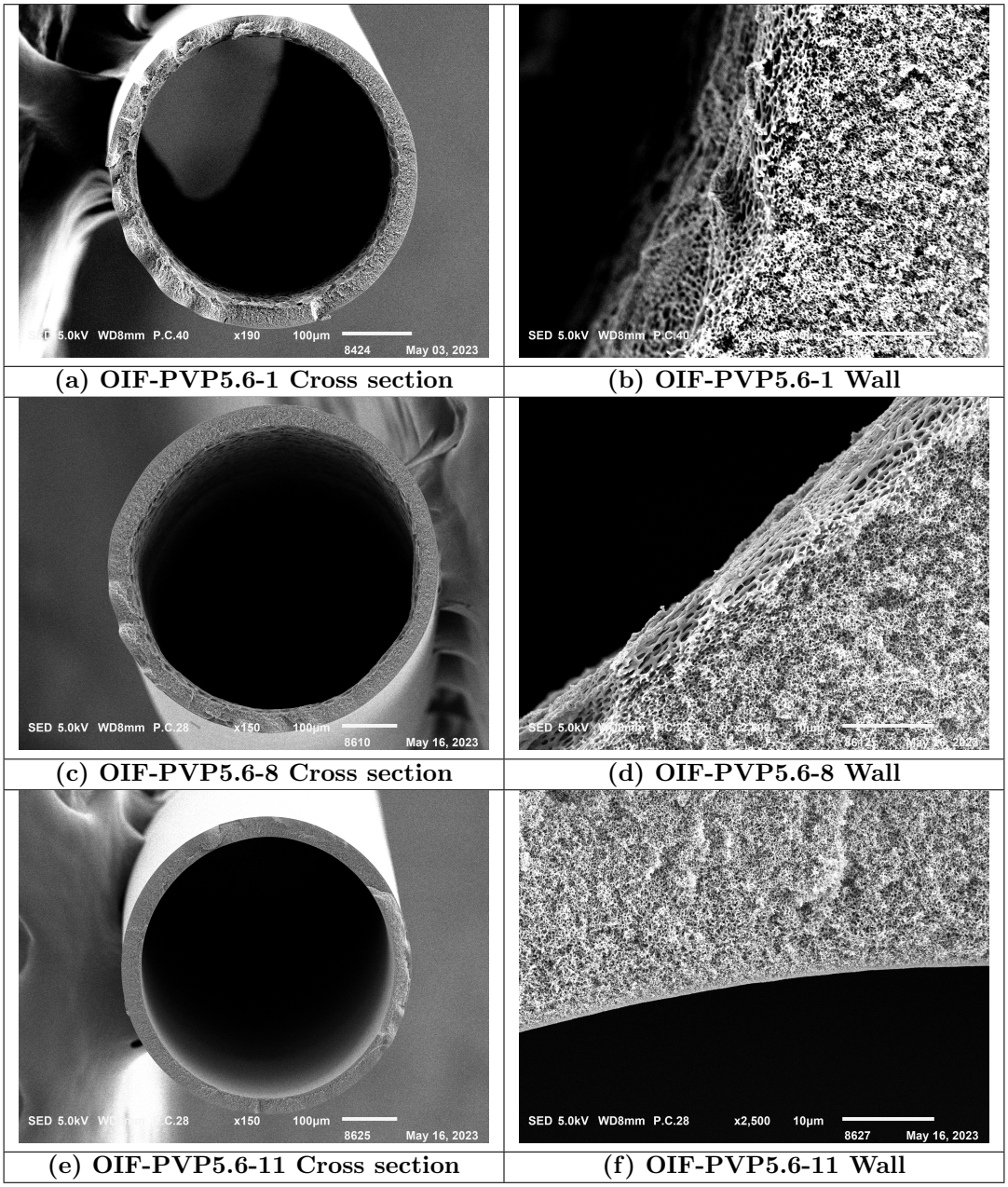

(a) OIF-PVP5.6-1 Cross section | **(b) OIF-PVP5.6-1 Wall**

(c) OIF-PVP5.6-8 Cross section | **(d) OIF-PVP5.6-8 Wall**

(e) OIF-PVP5.6-11 Cross section | **(f) OIF-PVP5.6-11 Wall**

Figure 10: SEM images of the OIF-PVP5.6 hollow fibers. **(a)** Cross section image OIF-PVP5.6-1 (190X) **(b)** Wall OIF-PVP5.6-1 (2500X) **(c)** Cross section image OIF-PVP5.6-8 (150X) **(d)** Wall OIF-PVP5.6-8 (2500X) **(e)** Cross section image OIF-PVP5.6-11 (150X) **(f)** Wall OIF-PVP5.6-11 (2500X)

Table 2: Measurements of the OIF-PVP5.6 hollow fibers using ImageJ compared to the preferred dimensions based on commercial fibers.

Fiber	OIF-PVP5.6-1	OIF-PVP5.6-8	OIF-PVP5.6-11	Preferred
Outer diameter (µm)	441	590	530	350
Inner diameter (µm)	365	530	460	270
Wall (µm)	31	40	40	40

Based on these results, it was stated that the produced fibers are not suited for dialysis. The dimensions of the fibers are not as they should be. The lumen of the fibers is too big and the walls are too thin, resulting in very unstable fibers. In this bachelor study, high flux single-layer outside-in fibers (OIF) composed of the hydrophobic PES polymer and hydrophilic PVP K90 polymer from a new

supplier, BASF, with N-Methyl-2-pyrrolidone (NMP) as solvent will be made, characterized and tested. The fibers produced in this study differ from the previous ones in terms of the PVP concentration. Instead of using a 5.6 wt.% PVP solution, a 4 wt.% PVP solution was used. The reason for this was to investigate the possibility of increasing the fiber strength and increasing the wall thickness. It was hypothesized that a larger volume of the dope solution needs to be pumped through the spinneret. Since the molecular weight of the PVP K90 polymer from BASF is higher than the PVP K90 from Sigma-Aldrich, this is challenging. Therefore, it was decided to decrease the PVP concentration from 5.6 to 4.0 wt.% to assess whether this modification leads to a lower viscosity of the dope solution. By reducing the viscosity, it is possible to pump a greater amount of the dope solution through the spinneret.

Additionally, by decreasing the PVP concentration, it is hypothesized that due to the lower hydrophilic properties of the dope solution, there will be slower movement of water present within the shower solution, bore solution and coagulation bath, creating a less sponge-like structured wall.

The advantage of using PVP K90 from BASF with a higher molecular weight than used previously, is that it could decrease the PVP elution. The longer PVP chains get entangled more with the PES chains, preventing the elution of PVP more.

1.6.1 Goal

Ultimately, the goal is to produce stronger fibers suited for the (long-term) toxin removal of patients' blood in OIF-mode with the preferred dimensions, displayed in table 2.

These dimensions are the ultimate goal since this allows for a greater quantity of fibers to be placed in the modules, making the dialyzer more efficient. The preferred water permeance ($L\,m^{-2}h^{-1}bar^{-1}$) of the fibers is at least 20 $L\,m^{-2}h^{-1}bar^{-1}$, which is the value for the filter to be a high-flux filter.

Previous studies with inhouse developed PES/PVP fibers for OIF dialysis (OIF-PVP5.6 [14]), have shown a creatinine removal in the range of 1500-2000 mg/m^2, after 4h. Therefore, in this study, a creatinine removal in the same range, or higher than this range is aspired.

Currently, there are a lot of commercial fibers used for dialysis present on the market. Fresinius Medical Care is one of the providers for commercial fibers used for dialysis. The commmercial FX high-flux dialyzers currently used express the toxin removal in clearance, given in $mL\,m^{-2}min^{-1}$. When looking at the toxin removal of the FX high-flux dialyzers for the inside-out modes, the clearance for creatinine ranges from 138 to 240 $mL\ m^{-2}\ min^{-1}$ [15]. In this study, not the clearance but the dialysance is calculated. The difference between these two is that for for clearance, the dialysis solution is refreshed constantly whereas for the dialysance, the dialysis solution is recirculated. It is preferred to recirculate the dialysis solution, since one therapy uses around 120 L of dialysis solution when constantly refreshing. If it is possible to do an effective toxin removal with recirculating the dialysis solution, only a few liters is necessary to perform the dialyse therapy [14]. Since this study is recirculating the dialysis solution, the dialysance of the fibers produced in this study will be compared to the clearance of the commercial fibers. It is preferred to have a similar, or even higher dialysance for the OIF-PVP4 hollow fibers compared to the clearance of the commercial fibers.

To be able to produce these fibers, a few steps into the right direction need to be made first to eventually achieve this goal. This study will make the first few steps to work further with in the future and produce fibers with the desired dimensions.

To spin the fibers, a fumehood-size spinning set-up is used which needs a spinning-protocol for these outside-in fibers. To characterize the fibers, the Scanning Electron Microscope (SEM) is used. To test the fibers, mini filters are prepared to mimic the dialyzer. For characterization and measuring filtration, the clean-water flux (CWF) set-up is used to determine the water permeance and ultrafiltration coefficient of the fibers. The Convergence set-up is used to perform a 4h dialysis experiment, using dialysis fluid and spiked human plasma with uremic toxins, creatinine (0.1mg/mL), to measure the toxin removal by these fibers.

2 Materials and Methods

2.1 Hollow fiber fabrication

2.1.1 Solutions

The solutions used for fiber spinning are the dope solution, the bore solution and the shower solution. As mentioned before, to obtain a selective outer layer, the shower solution will consists of 100% ultrapure water, the bore solution is a mixture of NMP and ultrapure water, starting with a 75/25% NMP/ultrapure water solution. For the dope solution, a solution composed of 12 wt.% hydrophobic polyethersulfone (PES)(ULTRASON, E6020P, BASF, Ludwigshafen, Germany), 4 wt.% hydrophilic polyvinylpyrrolidone (PVP)(Kollidon 90F, MW $\approx$ 1000.000 - 1500.000 Da, BASF, Ludwigshafen Germany) and 84 wt.% n-methyl-2-pyrrolidone (NMP) (Acros Organics, Belgium), acting as solvent, was made. The solution was put on a roller bank for 3 days to dissolve the polymers in the NMP. When dissolved, the solution was put in the stainless-steel syringe and hanged upside-down to degass overnight to get rid of air bubbles within the solution which could disturb the fiber spinning process, see figure 11.

As for the bore solution, the solution has been changed multiple times based on the results, resulting in fibers made with a bore solution of 75/25%, 63/37% and 50/50% NMP/ultrapure water solutions.

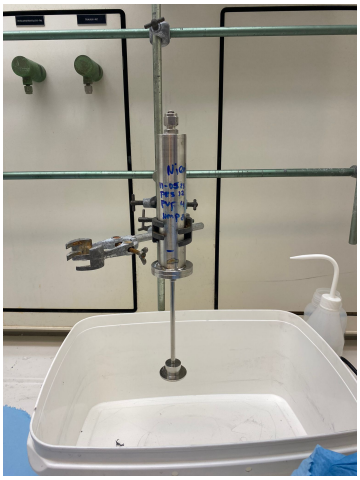

Figure 11: Syringe with the polymer solution for the outside-in fibers, upside-down for removal of air bubbles.

2.1.2 The spinneret set-up

To spin the fibers, the spinning set-up is used. The A85-0.2 spinneret is used to produce the hollow fibers. The dimensions of the spinneret used can be found in figure 12.

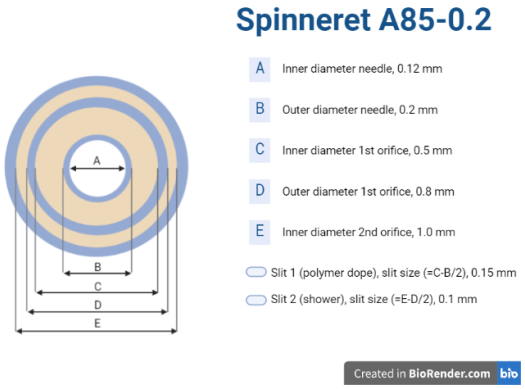

Figure 12: Composition of the spinneret.

The degassed dope solution was placed inside the pump located above the coagulation bath. The bore solution and shower solution are put inside a plastic syringe, placed inside the pumps and connected to the spinneret using 6mm polyethylene tubes, see figure 13 and 14. The pumps are necessary to regulate the liquid pumping speed ($m\,min^{-1}$) of all the solutions used.

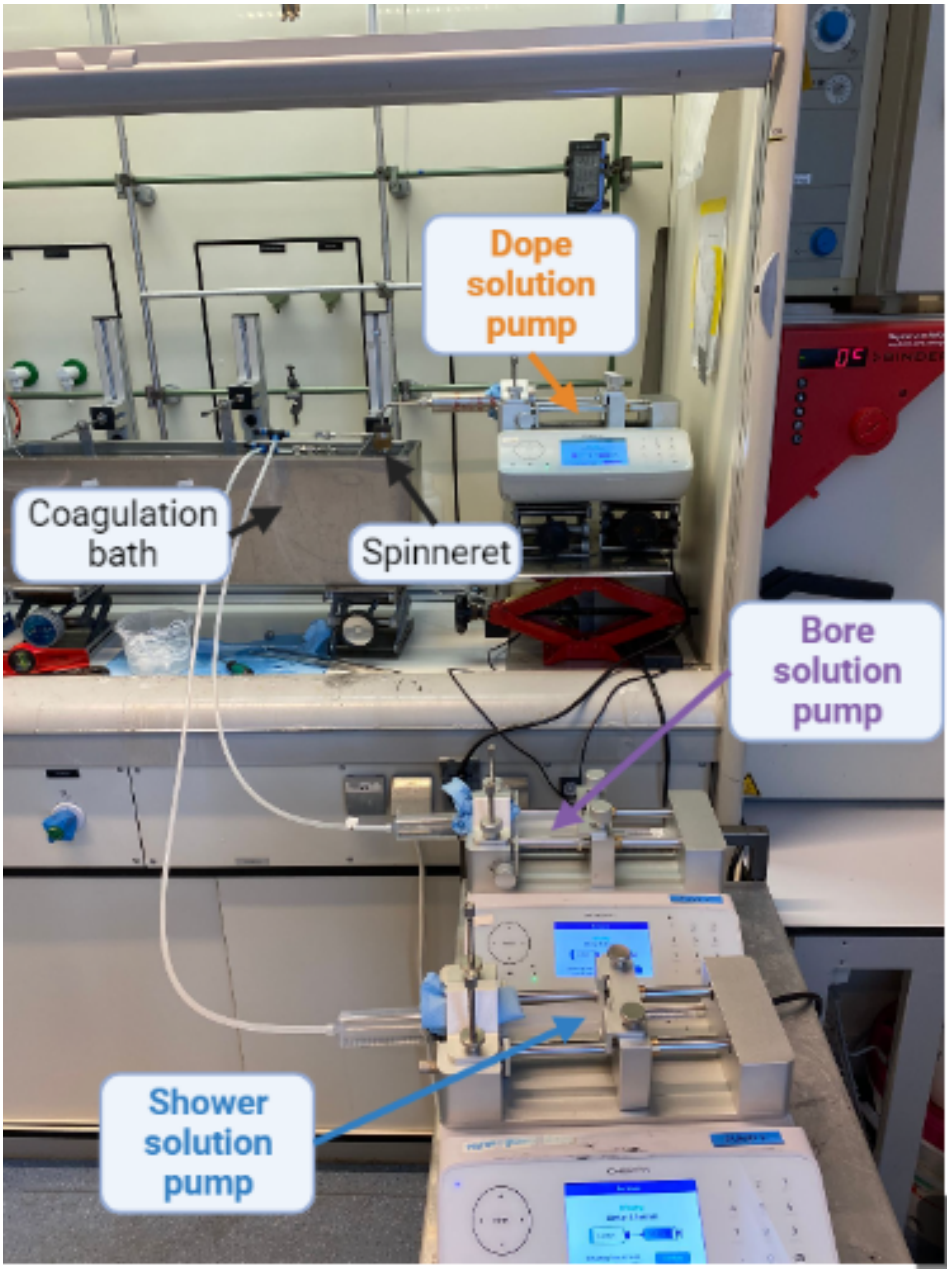

Figure 13: The solutions are placed in pumps and connected to the spinneret.

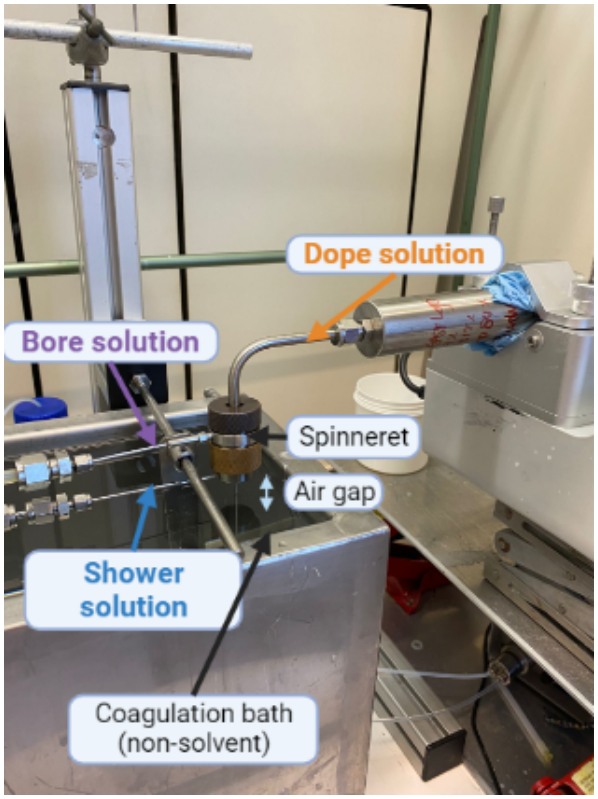

Figure 14: Solutions connected to the spinneret, placed above the coagulation bath.

The spinneret is positioned at the correct height above the coagulation bath to achieve the desired air gap, which in this case is 1.2 cm. Once the solution exits the spinneret, it spends a brief period within the air gap before entering the coagulation bath, which is filled with distilled water acting as non-solvent. To increase the time the fibers spend inside the coagulation bath, three wheels are placed inside the coagulation bath in a straight line with the spinneret and pulling wheel. The first and last wheel are placed at the bottom of the coagulation bath, whereas the second wheel is placed at the top of the coagulation bath. This configuration ensures that the fibers follow the longest path through the coagulation bath. Figure 15 shows the positioning of the wheels within the coagulation bath.

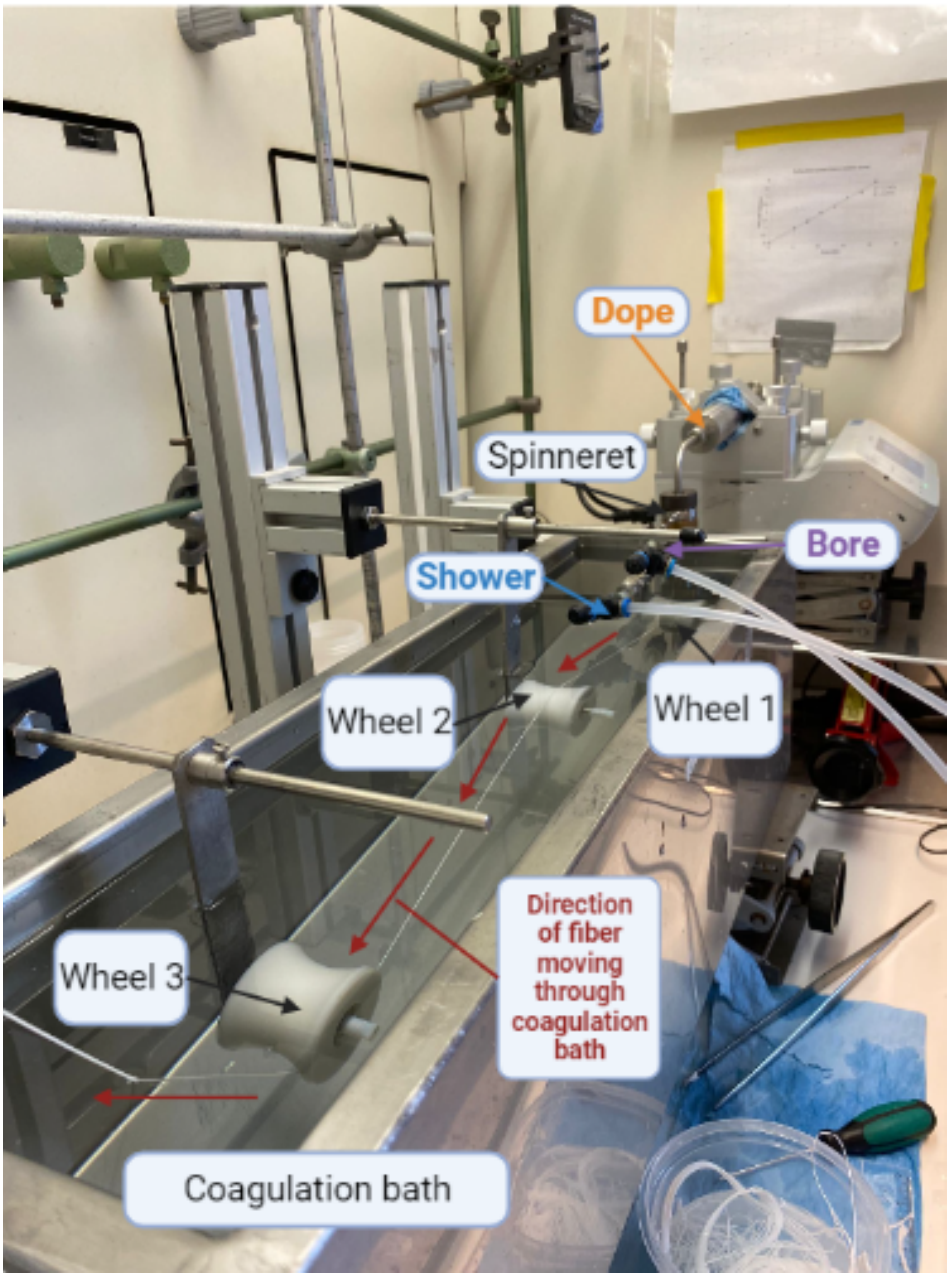

Figure 15: Positioning of the wheels within the coagulation bath.

After completing its journey through the coagulation bath, the fiber is placed on a pulling wheel and dropped inside a bucket filled with distilled water as non-solvent. The pulling wheel speed ($m\,min^{-1}$) can be adjusted by adjusting the voltage. The formula used for calculating the pulling wheel speed can be found in equation 1.

$$V_{wheel} = 5,4467 \cdot x - 8,0841 \tag{1}$$

In this study, pulling wheel speeds of 4.5 $m\,min^{-1}$ and 9.0 $m\,min^{-1}$ were used. By increasing the pulling wheel speed, more tension is placed on the fibers, resulting in thinner fibers. The pulling wheel speed is represented in figure 16.

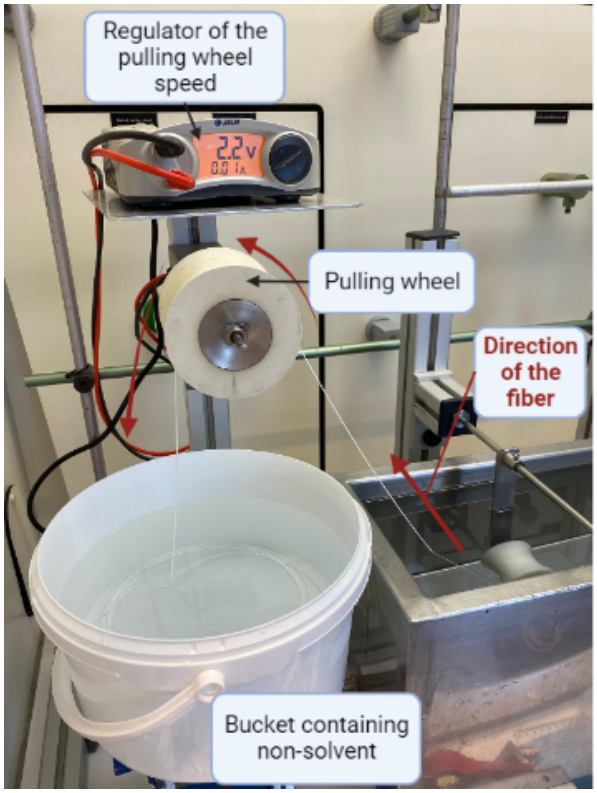

Figure 16: Representation of the pulling wheel.

After spinning the fibers, the non-solvent inside the bucket filled with the fibers is changed three times to make sure most NMP that is still exchanging with the water is removed. This is done to obtain stronger fibers and for safety reasons.

2.1.3 Spinning conditions

The spinning conditions used are displayed in table 3. The spinning conditions were based on the conditions used for the OIF-PVP5.6 hollow fibers and the resulting OIF-PVP4 hollow fibers.

Table 3: Spinning conditions of the OIF-PVP4 hollow fibers.

Parameters	OIF-PVP4-1	OIF-PVP4-2	OIF-PVP4-3
Dope pumping speed ($mL\,min^{-1}$)	1.8	1.0	1.0
Bore liquid pumping speed ($mL\,min^{-1}$)	1.3	0.4	0.2
Shower pumping speed ($mL\,min^{-1}$)	0.1	0.4	0.4
Air gap (cm)	1.2	1.2	1.2
Pulling wheel speed ($m\,min^{-1}$)	4.5	4.5	4.5
Bore solution (NMP/MilliQ)	75/25%	50/50%	50/50%
Shower solution	100% MilliQ	100% MilliQ	100% MilliQ

Parameters	OIF-PVP4-5	OIF-PVP4-6
Dope pumping speed ($mL\,min^{-1}$)	1.0	1.0
Bore liquid pumping speed ($mL\,min^{-1}$)	0.2	0.2
Shower pumping speed ($mL\,min^{-1}$)	0.4	0.4
Air gap (cm)	1.2	1.2
Pulling wheel speed ($m\,min^{-1}$)	4.5	9
Bore solution (NMP/MilliQ)	63/37%	63/37%
Shower solution	100% MilliQ	100% MilliQ

2.2 Preparation modules

The modules were prepared by placing 5 hollow fiber membranes within 6mm polyethylene tubes (PE tubes) (Bürkle, Germany) connected by push-in-T-connectors (Festo, The Netherlands). Two tubes of 4.5cm and one tube of 5.5cm were used to make one module. The 4.5cm tubes were placed at the outside of the module and the 5.5cm tube between the two T-connectors. To pot the modules, two-component Griffon combi fast glue (Klium, The Netherlands) was used and hardened overnight. The effective length of the module has a total length of approximately 10 cm, measured by measering the length between the glued borders on both sides of the filter. After drying, the fiber ends were cut off untill all fibers were open. Figure 17 shows a module after potting and figure 18 shows the open fibers after cutting off the fiber ends.

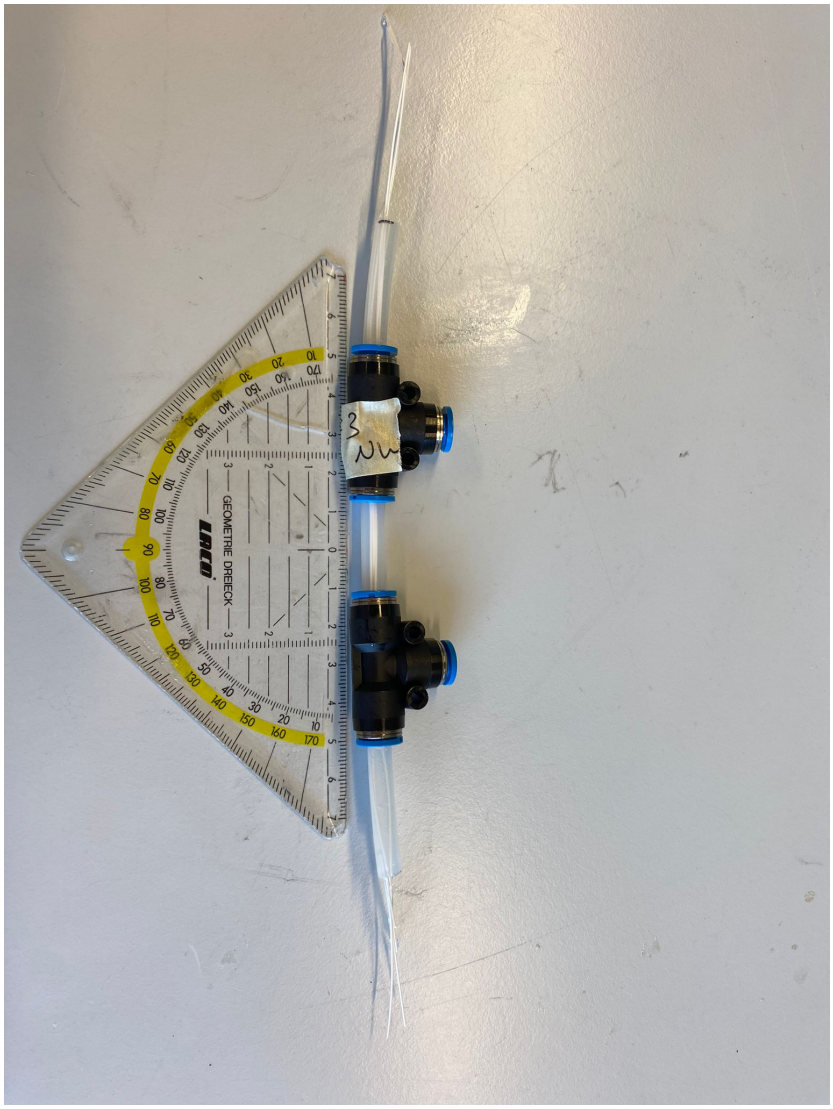

Figure 17: Module after potting the fibers

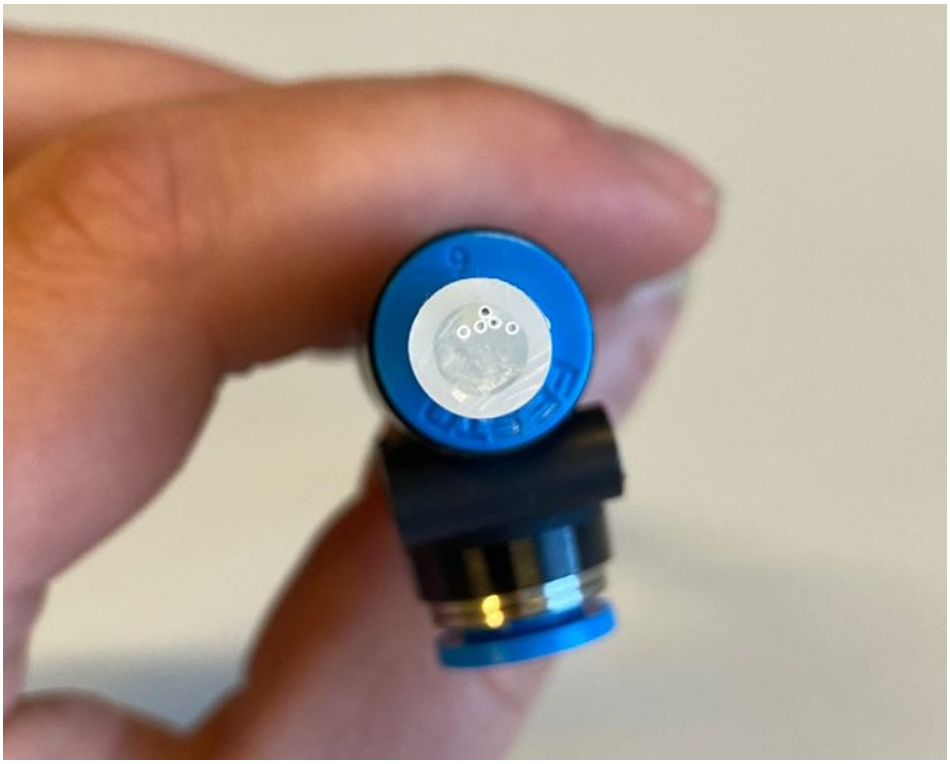

Figure 18: Cutted ends with all fibers open

2.3 Characterization of fibers

2.3.1 Scanning Electron Microscopy

A scanning electron microscope (SEM) (Jeol JSM-IT 100 LV, InTouchScopeTM software) was used to determine the morphology of the hollow fibers. The SEM uses electrons for imaging by shooting a gun of electrons into the sample under vacuum. The reflected or knocked off electrons of the sample surface are detected by detectors which form an image. The fibers made were examined to decide what fibers would be used for further testing or how the spinning process should be changed to achieve better fibers. First, the fibers were dried overnight at room temperature. To obtain SEM samples, a piece of fiber is put inside liquid nitrogen to freeze the fiber. When frozen, the fiber is broken into small pieces. These small pieces are placed in the cross-section holders by sticking the pieces of fibers on double-sided carbon tape which is placed on the cross-section holder. To analyze the dense outer-layer of the fibers, small pieces of fiber were placed on a 12 mm specimen holder with double-sided carbon tape. For analysis of the porous inner layer of the fibers, small pieces of fiber were shaved at the top of the fiber to have an 'open' fiber and be able to see the inside. These open fibers were also placed on a 12 mm specimen holder with double-sided carbon tape. The fiber samples were then sputter-coated with gold (Cressington 108 auto-sputter coater). Sputter coating with a conductive material is imperative to prevent the sample surface from charging, as this can lead to the production of unclear and unreadable images [16].

2.3.2 Clean water flux

Before using the fibers for measuring the toxin removal with the Convergence set-up, the permeability of the fibers was tested. This is done before measuring toxin removal, since the toxins in the plasma could clog the fibers and therefore have a lower permeability than unused fibers. To measure the permeability, the clean water flux (CWF) set-up was used. To connect the module to the CWF set-up, a push-in tap-connector (Festo, The Netherlands) was used. The other end of the module was blocked with a tap connector to regulate the water flow. Inside the vertical opening of the T-connectors, two 6 mm PE tubes were connected. The tube closest to the water entrance was blocked by adding a stop. The water used is ultrapure water which is purified by the Milli-Q® Direct Water Purification

System (Merck Millipore, Czech Republic). By pushing ultrapure water through the fibers on one end, and blocking the other end, the water is forced through the pores of the fiber walls and drips through the open 6 mm PE tube. The water permeability is then found by measuring how much water was forced through the fibers at a certain pressure over a certain membrane surface area and over a certain time. This experiment is called dead-end filtration. Figure 19 shows the dead-end filtration experiment set-up.

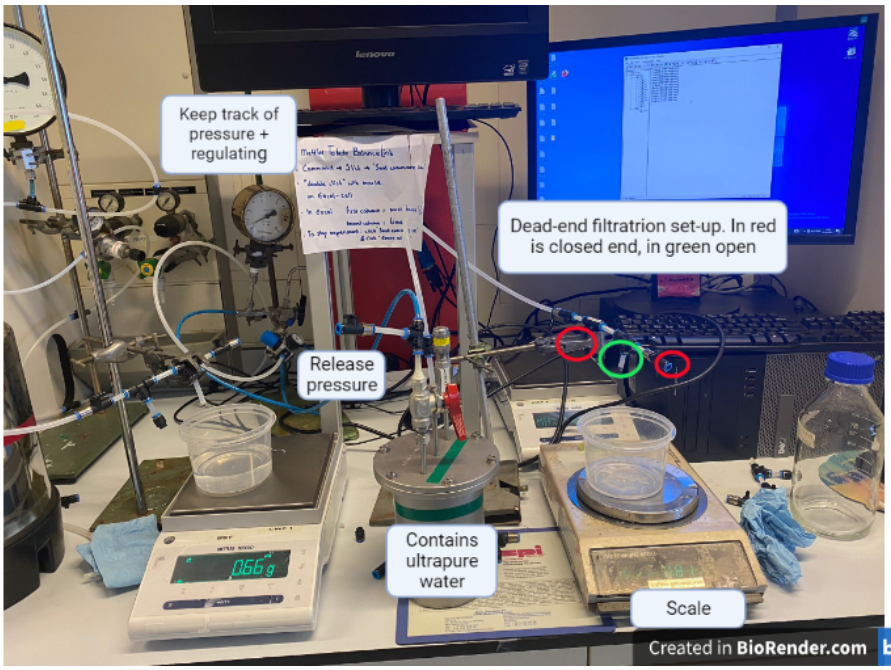

Figure 19: Set-up for measuring the water permeance using the dead-end filtration experiment.

The measurements for 1 module were done at 3 different pressures, 0.6, 0.4 and 0.2 bar, measuring 30 min for each pressure starting with highest pressure as a pre-compaction step. After measuring all the wanted pressures, the highest pressure is once again measured to check if the permeability is still around the same value and to know for sure the true value. The flux (L/m^2 h) is then calculated by using equation 2. The mass is converted to the Volume (V) in liters and divided by measurement time (t) in hours to calculate the flow (L/h). The flow is then divided by the total effective surface area of the module (A_{eff}), calculated using equation 3, to find the flux [17].

$$Flux = \frac{V}{A_{eff} \cdot t} \tag{2}$$

$$A_{eff} = 2 \cdot \pi \cdot r \cdot L \cdot n \tag{3}$$

Here, r is the radius of the fiber, L the effective length of the fibers and n the number of fibers inside the module. To determine the radius used in Equation 3, an analysis of the Scanning Electron Microscopy (SEM) cross-section images is performed. By measuring the diameter of the outer layer of the fiber up to the selective layer and dividing this diameter by two, the corresponding radius (r) is obtained. When the fluxes are calculated, the flux is plotted as a function of pressure. A linear relation between flux and pressure is expected. Therefore, the slope of this linear graph gives the water permeance of the fibers in $L\, m^{-2} h^{-1} bar^{-1}$.

2.3.3 NaOCl treatment

If the flux measured is too low, the fibers are bleached with sodium hypochlorite (NaOCl). Chlorine oxidizes the membrane polymer, especially the pore forming polymers such as PVP. The hypochlorite treatment changes the membrane characteristics due to degradation and leaching of PVP from the membrane. The mechanisms responsible for this degradation is polymer chain scission and opening

of the pyrrolidone ring of the PVP. Previous studies showed that treatment with 4000-6000 ppm hypochlorite can change the flux by 4-5.4 times and changes the effective pore size of the membrane [18][19]. It should be taken into consideration that the sodium hypochlorite could change the membrane properties. By washing away some of the PVP, the fiber will become less hydrophilic. This increases the chance of membrane fouling. In addition, it is a possibility that some of the sodium hypochlorite is not washed away properly after the bleaching process and washing steps. Therefore, the flux is measured first without bleaching and the membranes are only treated with hypochlorite when necessary [18][19].

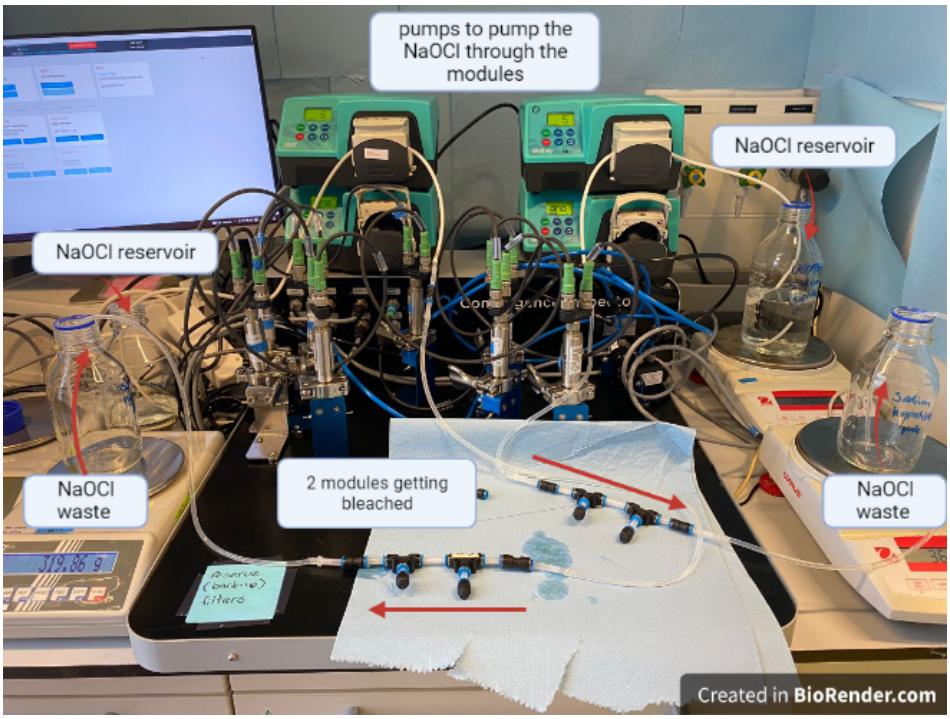

Figure 20: Bleaching the modules using the Convergence set-up.

2.3.4 Toxin removal

Dialysate In this experiment, dialysis solution flows within the fibers' lumen and is necessary to remove toxins from the human plasma. This dialysis solution needed to be made first. Considering approximately 100 mL dialysis solution flows through one module, 1000 mL was made to make sure there is enough. The dialysis solution used for measuring the toxin removal consists of multiple components; Potassium chloride (KCl, 0.146mg/mL), sodium chloride (NaCl, 8.158mg/mL), calcium chloride ($CaCl_2$, 0.224mg/mL), magnesium chloride ($MgCl_2$, 0.024mg/mL), sodium bicarbonate ($NaHCO_3$, 2.945mg/mL) (Sigma-Aldrich, Germany) and glucose (0.984mg/mL) (Life Technologies Europe BV, The Netherlands). These substances were added to 1000 mL ultrapure water and stirred at 300 RPM at room temperature to dissolve. The pH was then adjusted to approximately 7.4 by adding 1M HCL (Sigma-Aldrich, Germany) and stored at -20°C for further use.

Blood plasma For measuring the toxin removal, a solution needed to be made to mimic blood. Human plasma obtained from healthy donors (Sanquin, The Netherlands) was warmed first to 37°C in a water shaking bath at 50 RPM. The plasma is then filtered by using a strainer (Greiner bio-one Easy Strainer TM 70um sterile, CATnr 542-070). 2x1 mL of unspiked, filtered plasma is put into two Eppendorf's for analysis with ultraviolet-visible spectrophotometer (UV-Vis) and put in the freezer at -20°C for later use. After filtering, the plasma is spiked with 0.1mg/mL creatinine (113 Da) (Sigma-Aldrich, The Netherlands) and stirred for 1h at 200 RPM. After stirring, the spiked plasma is put in the shaking water bath for 4h at 50 RPM at 37°C. When cooled down, the flask was put in the freezer at -20°C for later use.

Convergence set-up To measure the toxin removal, the Convergence set-up (Convergence inspector, Enschede, The Netherlands) is used. The set-up used for cross-flow filtration in outside-in mode is seen in figure 21. The set-up consists of four pressure detectors, two pumps and 2 scales. To perform counter-current outside-in filtration, the end of the module with the open fibers is connected to 100 mL dialysis fluid, which flows from left to right with a flow of 10 mL/min. 50 mL spiked human plasma is connected to the vertical T-connector on the right side, and flows from right to left through the inter-fiber space with a flow of 1 mL/min, see figure 22. Both plasma and dialysis fluid recirculate.

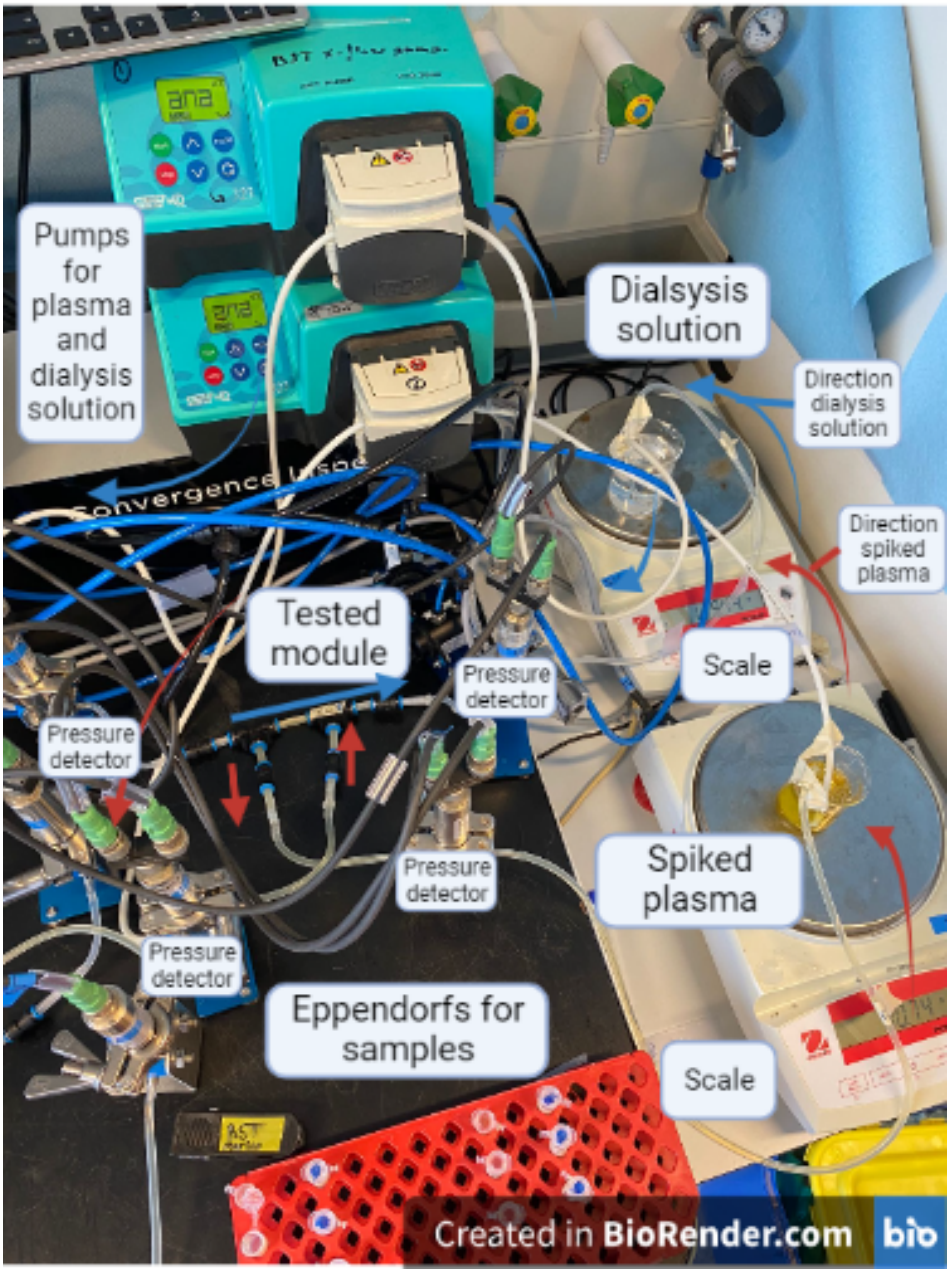

Figure 21: Performing a toxin removal experiment using the Convergence set-up.

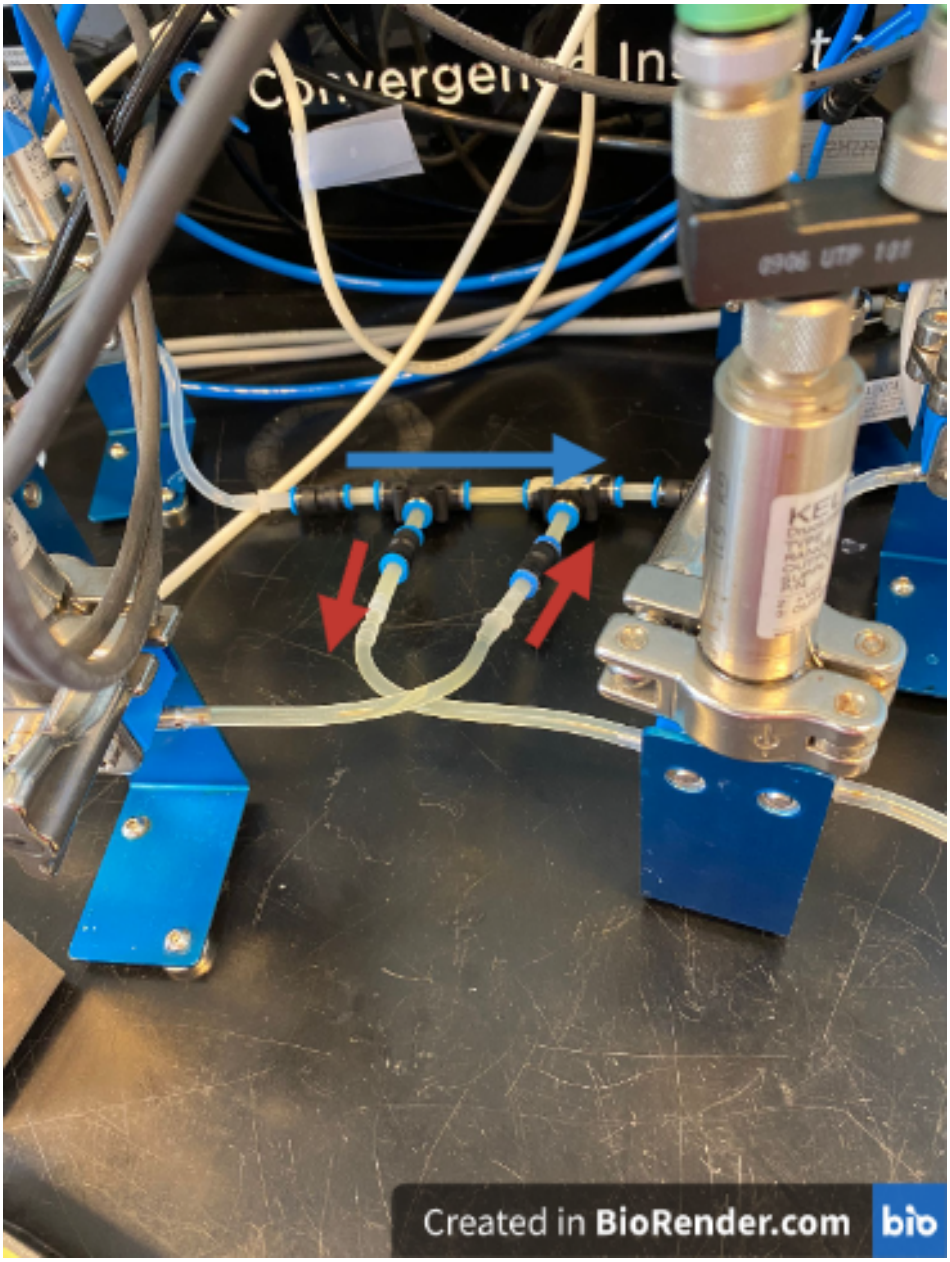

Figure 22: Zoom-in blood and dialysis flow through module during toxin removal experiment.

To observe changes in toxin removal, samples of 1 mL were taken at t=0, t=30, t=60, t=120, t=180 and t=240, with t in minutes from both plasma and dialysis fluid. The mass of the plasma and dialysis was also measured before and after taking a sample to check if fluid or other particles moved from one fluid to the other fluid. The TMP is also measured before and after taking the sample to ensure a TMP around 0. After the measurements, the tubes were cleaned with ultrapure water for 30 min, 30 minutes with ethanol and another 30 min with ultrapure water.

2.4 UV-Vis

To measure the removal of creatinine, the Nanodrop (ND-1000 Specrophotometer, Fisher Scientific) is used. The concentration of creatinine present in the 1 mL samples of the dialysis fluid and the human plasma are measured by measuring the absorbed light by creatinine present in both plasma and dialysis fluid. Ultraviolet–visible spectrophotometry (UV-VIS) is used for measuring the creatinine with the nanodrop. Before measuring the plasma samples, 100 µL of each plasma sample was put inside a

amicon 0.5 mL ultra centrifugal filter and placed inside the centrifuge at 14000 rpm for 15 min to remove the albumin present within the plasma samples. The dialysate samples are not filtered.

To measure the creatinine concentration, 2 µL of ultrapure water is dropped onto the detector followed by the t0 of the dialysis fluid to set a blank. All samples are then measured by dropping 2 µL on the detector, closing the lid and make the measurements two times for every sample. If the values differ too much, more measurements were done. In between every measurement, both the detector and the lid were cleaned with a dry tissue. After measuring the dialysate fluid samples, the plasma samples are measured in the exact same way, but now using the unspiked plasma sample as a blank. All measurements were done at $\lambda = 235$ nm.

Besides measuring the concentration creatinine present, a calibration curve was made to determine the relationship between the absorbance and concentration creatinine. The t0 sample of plasma was diluted 3 times to obtain 0.1mg/mL, 0.05mg/mL, 0.025mg/mL and 0.0125mg/mL creatinine. These dilutions were also measured with the nanodrop, analyzed and used to calculate the creatinine removal of the modules in mg/m^2.

Dialysance To be able to compare the results to the commercial fibers, the dialysance for both the plasma and the dialysate (both $mL\, m^{-2}\, min^{-1}$) was calculated using the equation 4 for the plasma and equation 5 for the dialysate.

$$DL_p = \frac{\frac{X_p}{t \cdot A_{eff}}}{(C_p - C_d)} \tag{4}$$

$$DL_d = \frac{\frac{X_d}{t \cdot A_{eff}}}{(C_p - C_d)} \tag{5}$$

where X_p is the amount of toxins removed from the plasma and X_d is the amount of toxins transported to the dialysis solution (mg) after a certain time t (min). A_{eff} is the effective surface area of the module (m^2). C_p and C_d (both $mg\, mL^{-1}$) are the concentrations of the toxins in the plasma and in the dialysis solution. The dialysance calculates the toxin removal when the dialysis solution is recirculated, which is the case in this study [13].

3 Results and Discussion

3.1 Hollow fiber OIF-PVP4-1

In order to compare the characteristics of fibers containing 4 wt.% PVP and 5.6 wt.% PVP, both K90 from BASF, the spinning conditions for the 4 wt.% PVP fibers were kept consistent with those used for the previously produced OIF-PVP5.6 hollow fibers. The pulling wheel speed used was 4.5 m/min to achieve stronger and thicker fibers, as the prior 5.6 wt.% PVP fibers were too weak and thin and the 9 m/min pulling wheel speed could cause this again. For both fiber types, the bore solution consisted of 75% NMP and 25% ultrapure water. Despite these similarities in the spinning conditions, the fibers containing 4 wt.% PVP did not successfully form. These fibers appeared excessively thin, were transparent in the coagulation bath, and frequently experienced breakage. Attempts were made to tackle this issue by altering the spinning parameters, as detailed in table 4.

Table 4: Spinning conditions of the OIFPVP5.6 hollow fibers and the OIF-PVP4-1 hollow fibers.

Parameters	**OIF-PVP5.6-1**	**OIF-PVP4-1**
Dope pumping speed ($mL\,min^{-1}$)	1.0	1.8
Bore liquid pumping speed ($mL\,min^{-1}$)	0.4	1.3
Shower pumping speed ($mL\,min^{-1}$)	0.4	0.1
Air gap (cm)	1.2	1.2
Pulling wheel speed ($m\,min^{-1}$)	9	4.5
Bore solution (NMP/MilliQ)	75/25%	75/25%
Shower solution	100% MilliQ	100% MilliQ

Although these modifications led to the formation of small fiber fragments, the fibers remained prone to breakage due to the interference of the shower dripping onto the fiber. The resulting appearance of the fibers resembled a necklace of pearls, see figure 23. A small piece of this pearl necklace looking fiber was analysed with the SEM, displayed in figure 24.

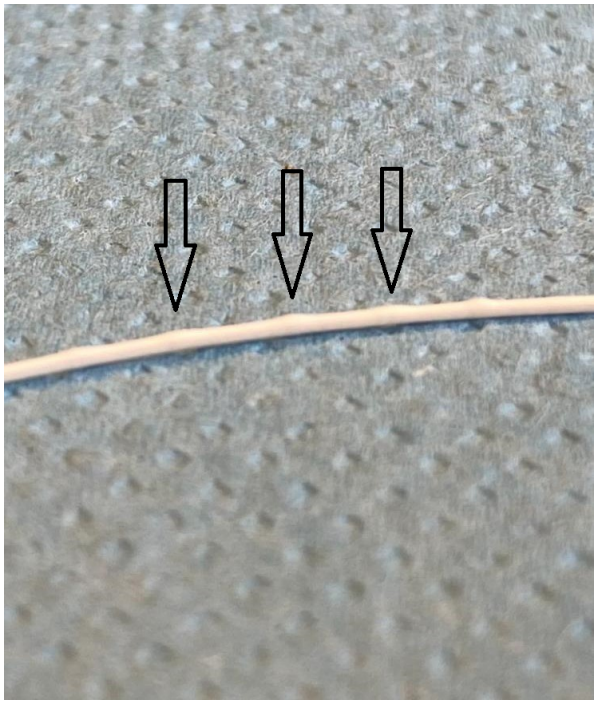

Figure 23: OIF-PVP4-1 hollow fibers, resembling a pearl necklace.

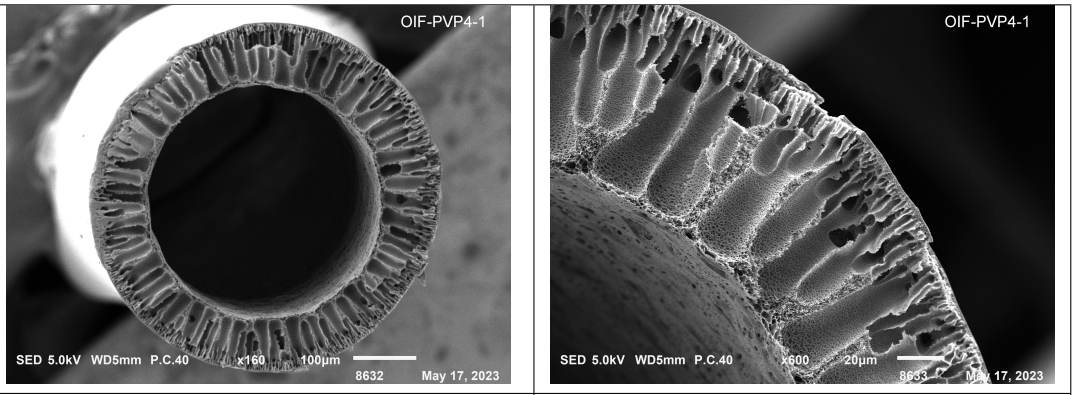

(a) OIF-PVP4-1 Cross section | **(b) OIF-PVP4-1 Wall**

(c) OIF-PVP4-1 Inner + outer surface | **(d) OIF-PVP4-1 Outer surface**

Figure 24: SEM images of OIF-PVP4-1 hollow fibers, **(a)** Cross section image (160X) **(b)** Wall (600X) **(c)** Inner + outer surface (180X) **(d)** Outer surface (110X)

Table 5: Measurements of the OIF-PVP4-1 hollow fiber using ImageJ. Note that only a small piece of the heteregeneous fiber was obtained.

Fiber	OIF-PVP4-1
Outer diameter (µm)	557
Inner diameter (µm)	375
Wall (µm)	91

Remarkably, despite the initial difficulties encountered with the fibers containing 4 wt.% PVP, some promising characteristics were observed in the formed fibers. These fibers exhibited a dense outer layer and a porous inner layer, along with a finger-like macrovoid structure within the wall, see figure 24 (b), (c) and (d). The macrovoid-structured wall indicates that the 4 wt.% PVP is indeed slowing down the pore formation. These findings provide encouragement for further exploration and production of fibers using 4 wt.% PVP. Since the fibers stayed transparent in the coagulation bath during the spinning process, it was hypothesized that the phase exchange between water and NMP was too slow. To obtain a faster phase exchange, the difference between the NMP within the dope solution and the water within the bore solution needs to be bigger. Therefore, the bore solution was changed from 75/25% to a 50/50% NMP/ultrapure water solution. Since the fiber did have a dense outer layer, it was concluded that the shower solution being 100% ultrapure water is indeed the shower solution necessary for the OIF-PVP4 hollow fibers and was therefore kept the same for the further produced fibers.

3.2 Hollow fiber OIF-PVP4-2 & OIF-PVP4-3

A new bore solution consisting of a 50/50% mixture of NMP and ultrapure water was used. The same parameters used for the previous production of 5.6 wt.% PVP fibers were used for comparison. During the spinning process with this modified bore solution, a notable observation was made: the fibers formed instantly, did not break anymore due to interference with the shower and were no longer transparent, but white. This observation suggests that for the lower PVP percentage fibers, either a higher concentration of ultrapure water or a lower concentration of NMP in the bore solution is required to facilitate faster phase separation with the dope solution and thus better fiber formation. In addition to the bore solution adjustment, the bore liquid pumping speed was adjusted by reducing it from 0.4 mL/min to 0.2 mL/min. This modification aimed to promote the production of thicker fibers. An overview of the spinning conditions can be found in table 6.

Table 6: Spinning conditions for the OIF-PVP4-2 hollow fibers and the OIF-PVP4-3 hollow fibers.

Parameters	OIF-PVP4-2	OIF-PVP4-3
Dope pumping speed ($mL\,min^{-1}$)	1.0	1.0
Bore liquid pumping speed ($mL\,min^{-1}$)	0.4	0.2
Shower pumping speed ($mL\,min^{-1}$)	0.4	0.4
Air gap (cm)	1.2	1.2
Pulling wheel speed ($m\,min^{-1}$)	4.5	4.5
Bore solution (NMP/MilliQ)	50/50%	50/50%
Shower solution	100% MilliQ	100% MilliQ

The scanning electron microscopy (SEM) images illustrating the resulting fibers are presented in Figure 25.

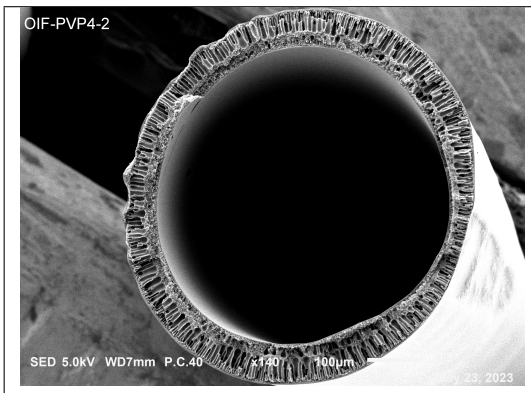

(a) **OIF-PVP4-2 Cross section**

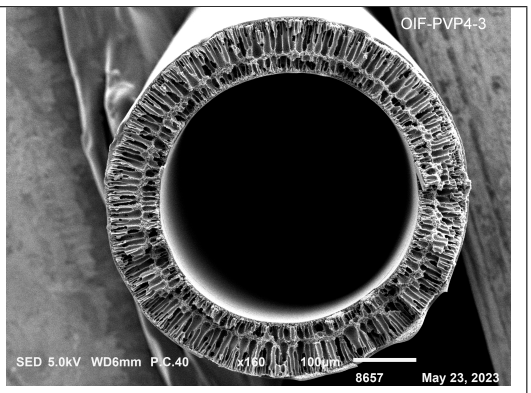

(b) **OIF-PVP4-3 Cross section**

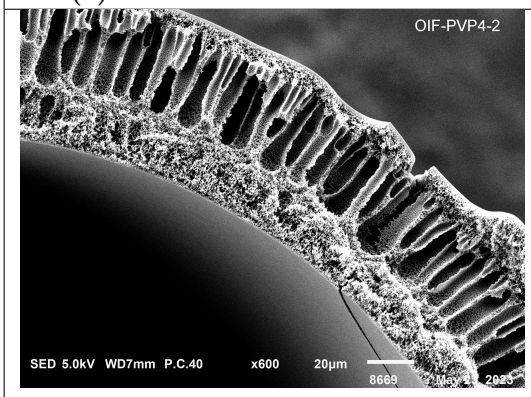

(c) **OIF-PVP4-2 Wall**

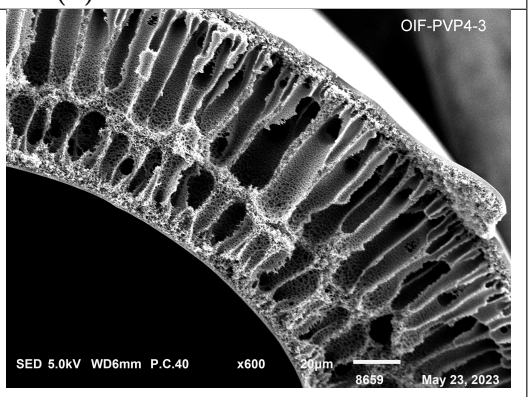

(d) **OIF-PVP4-3 Wall**

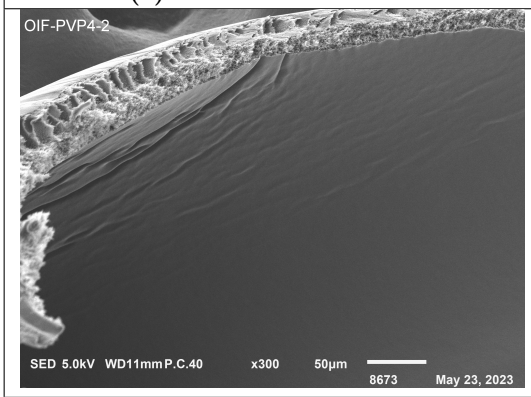

(e) **OIF-PVP4-2 Inner surface**

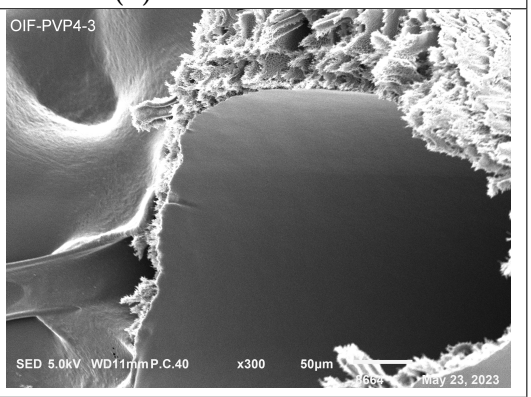

(f) **OIF-PVP4-3 Inner surface**

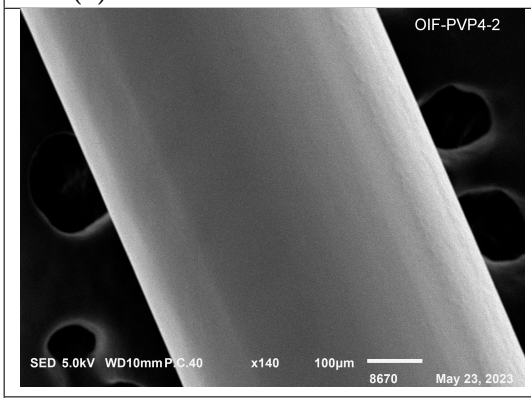

(g) **OIF-PVP4-2 Outer surface**

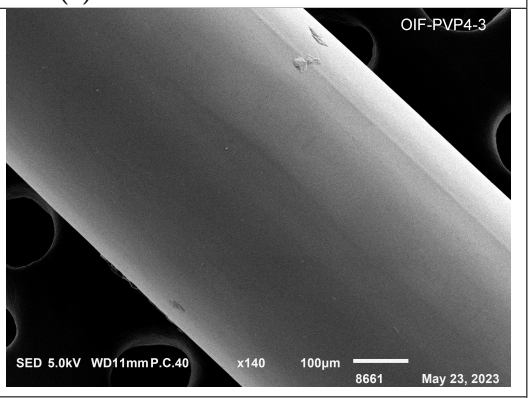

(h) **OIF-PVP4-3 Outer surface**

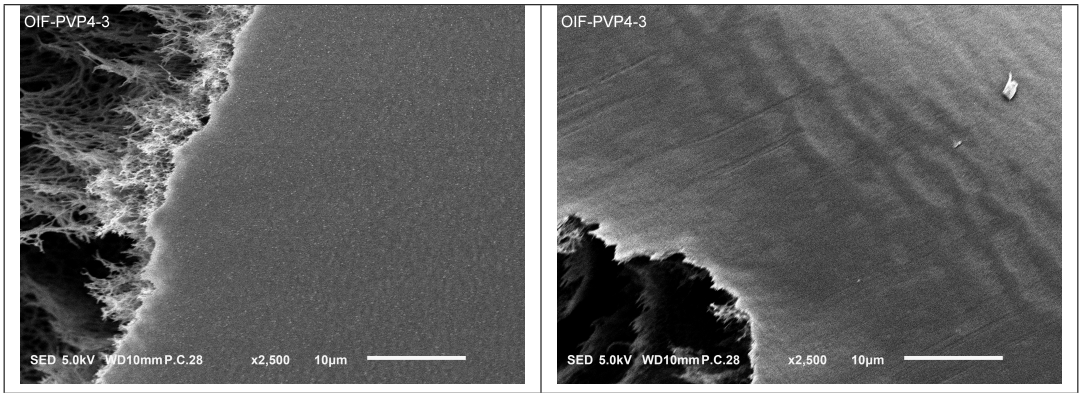

(i) OIF-PVP4-3 Inner surface | **(j) OIF-PVP4-3 Outer surface**

Figure 25: SEM images of OIF-PVP4-2 and OIF-PVP4-3 hollow fibers, **(a)** Cross-section OIF-PVP4-2 (140X) **(b)** Cross-section OIF-PVP4-3 (160X) **(c)** Wall OIF-PVP4-2 (600X) **(d)** Wall OIF-PVP4-3 (600X) **(e)** Inner surface OIF-PVP4-2 (300X) **(f)** Inner surface OIF-PVP4-3 (300X) **(g)** Outer surface OIF-PVP4-2 (140X) **(h)** Outer surface OIF-PVP4-3 (140X) **(i)** Inner surface OIF-PVP4-3 (2500X) **(j)** Outer surface OIF-PVP4-3 (2500X)

Table 7: Measurements of the OIF-PVP4-2 and OIF-PVP4-3 hollow fibers using ImageJ.

Fiber	OIF-PVP4-2	OIF-PVP4-3
Outer diameter (µm)	678	584
Inner diameter (µm)	537	401
Wall (µm)	70	92

Notable differences between the two fibers became apparent, particularly when considering the cross-sections. The fiber produced under the initial spinning conditions has a relatively thin and non-homogeneous layer, while the fiber created using the reduced bore liquid pumping speed displayed a thick and uniform wall. In addition, it is observed that the fiber wall of the OIF-PVP4-2 hollow fiber has a finger-like macrovoid layer and a sponge-like layer whereas the OIF-PVP4-3 hollow fiber has two finger-like macrovoid layers. This indicates that the decrease in the bore liquid pumping speed leads to a slower exchange between the NMP present in the dope solution and the water within the bore solution, resulting in less small pores formed. Consequently, the bore solution was maintained at this lower pumping speed for the subsequent fibers. Both fibers exhibited a finger-like macrovoid-structured wall and a smooth, dense outer layer. However, a significant change was observed in the inner surface of these fibers compared to those produced using the 75/25% NMP/ultrapure water bore solution. Instead of a highly porous inner layer, the inner region now has a big resemblance to the outer layer, displaying a smooth and dense composition. This raised the question of whether a porous inner layer actually existed or if the inner region is the same as the outer layer, having a continuous, dense layer throughout as a result of the faster exchange between the NMP present in the dope solution and the water within the bore solution.

3.2.1 Water permeance OIF-PVP4-3

The water permeance of the OIF-PVP4-3 fiber was measured. This selection was made due to its superior mechanical properties compared to the OIF-PVP4-2 fiber. Three modulus containing 5 fibers were made to measure the water permeance ($L\,m^{-2}h^{-1}bar^{-1}$) of the fiber membranes (n=3). The result is displayed in figure 26.

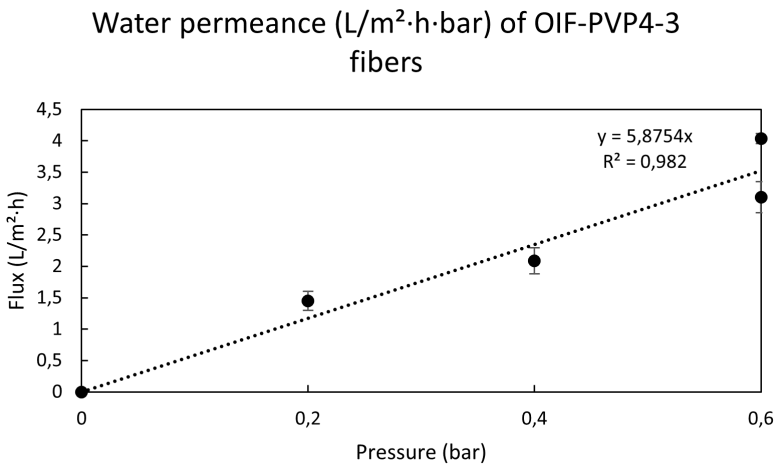

Figure 26: Water permeance measured for hollow fiber OIF-PVP4-3 (n=3). The slope of the graph represents the water permeance ($\approx 6\ L\,m^{-2}h^{-1}bar^{-1}$).

The figure shows two values for the flux at 0.6 bar. This is because the water permeance was measured twice at 0.6 bar in order to open all the fibers. The lowest dot represents the first measurement done at 0.6 bar, while the highest dot represents the last measurement done at 0.6 bar. It can be clearly seen that the flux did indeed increase after opening up the pores first. Unfortunately, the water permeance value was found to be quite low, falling outside the desired value of $\geq 20\ L\,m^{-2}h^{-1}bar^{-1}$. The OIF-PVP4-3 fiber exhibited a water permeance of $\approx 6\ \pm\ 2\ L\,m^{-2}h^{-1}bar^{-1}$. The low water permeance of the fiber membranes indicate that the pores are too small, which will eventually result in a low toxin removal. In order to increase the water permeance values of the fiber membranes, a sodium hypochlorite treatment was performed.

3.2.2 Water permeance OIF-PVP4-3 after NaOCl treatment

To increase the permeability of the fibers, the fibers were bleached with 4000 PPM sodium hypochlorite (NaOCl). The bleach used was a mixture of 4000 parts-per million (PPM) 12.5% sodium hypochlorite with MilliQ water. After the NaOCl treatment, the water permeance for all three modules were measured again (n=3). The result is displayed in figure 27.

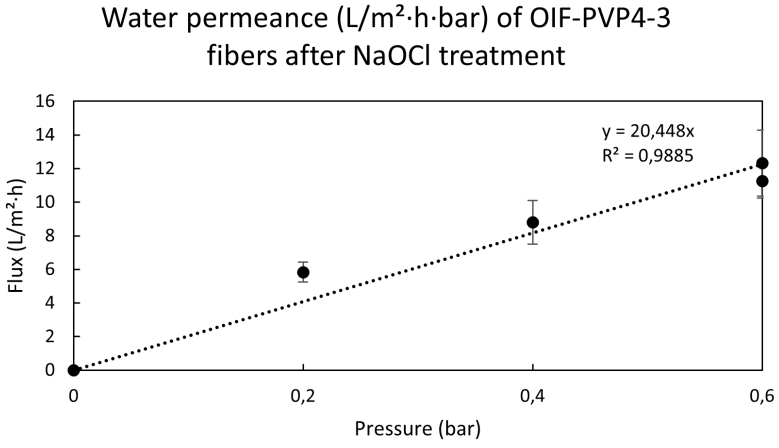

Figure 27: Water permeance measured for hollow fiber OIF-PVP4-3 after the NaOCl treatment (n=3). The slope of the graph represents the water permeance ($\approx 20\ L\,m^{-2}h^{-1}bar^{-1}$).

As a result of the NaOCl treatment, the water permeance increased to a value of $\approx 20\ \pm\ 5$

$L\,m^{-2}h^{-1}bar^{-1}$, which is almost 4 times as high as the previously measured water permeance and does fall within the desired value of $\geq 20\ L\,m^{-2}h^{-1}bar^{-1}$. The increase in water permeance is a result of washing away some of the PVP present within the fiber wall. By washing away the PVP, the pores of the fiber increase and allow more water to move through the fiber wall.

3.2.3 Toxin removal OIF-PVP4-3

For measuring the toxin removal, healthy human plasma was spiked with 0.1mg/mL creatinine and a cross-flow filtration in outside-in mode was performed using the Convergence set-up (n=3). The results of the modules tested are displayed in figure 28.

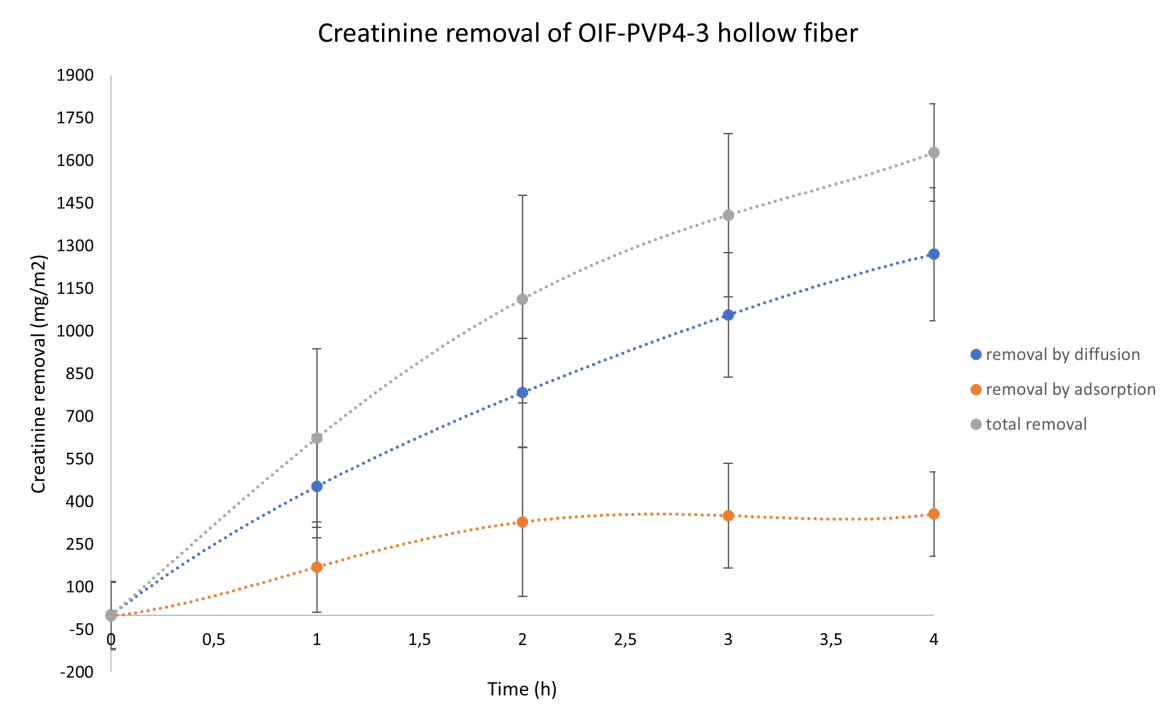

Figure 28: Creatinine removal for the OIF-PVP4-3 fiber (n=3). The total removal, removal by diffusion and removal by adsorption are measured ($mg\,m^{-2}$).

The removal is approximately 1630 ± 171 $mg\,m^{-2}$ after 4h, which does fall within the creatinine removal range of 1500 - 2000 mgm^{-2} after 4h, which is the creatinine removal range of the OIF-PVP5.6 hollow fibers made with PVP K90 from Sigma-Aldrich. The figure shows that most of the creatinine removed from the plasma is because of diffusion, being 1271 ± 234 $mg\,m^{-2}$ after 4h. This indicates that the toxins indeed move from the selective layer into the dialysis solution while only a small part is absorbed by the fiber wall. Because of the relatively small toxin absorption, the fiber membrane is less sensitive to membrane fouling.

The dialysance was calculated using the slope presented in figure 29.

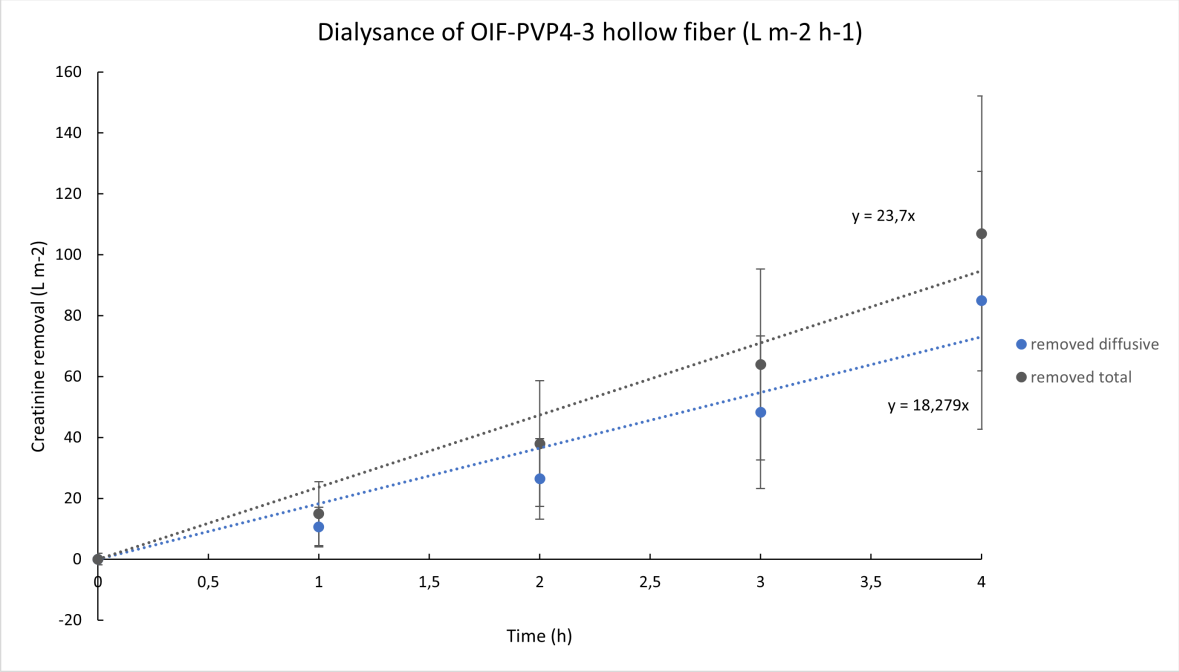

Figure 29: Dialysance of creatinine for the OIF-PVP4-3 fiber (n=3). The total removal and removal by diffusion are measured ($L\,m^{-2}\,h^{-1}$).

The slope of both the total removal as well as the removal by diffusion represent the dialysance in $L\,m^{-2}\,h^{-1}$. The total dialysance is approximately 24 $L\,m^{-2}\,h^{-1}$, with approximately 18 $L\,m^{-2}\,h^{-1}$ because of diffusion. To compare these results to the FX high-flux dialyzers, the dialysance was converted to $mL\,m^{-2}\,min^{-1}$, giving a total dialysance of approximately 395 $mL\,m^{-2}\,min^{-1}$ with approximately 305 $mL\,m^{-2}\,min^{-1}$ of the dialysance because of diffusion. This dialysance is bigger than the clearance of the FX high-flux dialyzers from Fresenius (FX40, FX50, FX60, FX80 FX100) , which ranged from 138 to 240 $mL\,m^{-2}\,min^{-1}$. However, it is important to consider that the calculated clearance values for the FX high-flux dialyzers are based on blood clearance rather than plasma clearance. Filtering blood is a greater challenge than filtering plasma, suggesting that if blood had been utilized in this study, the observed dialysance could have been significantly lower. Moreover, there are variations in flow rates between both experiments, which may have influenced the results as well. This study used a flow rate of 1 mL/min for the plasma and 10 mL/min for the dialyis solution, whereas for the FX high-flux dialyzers from Fresenius, the flow rates used for blood were 200 mL/min, 300 mL/min and 400 mL/min and the flow rate for the dialysis solution was 500 mL/min. This means that the ratio between the flow rate of the plasma and the dialysis solution of this study are not in line with the ratios used between the blood and dialysis solution for the FX high-flux dialyzers from Fresenius.

Another difference lies in the fiber housing used: the FX high-flux dialyzers contain approximately 10.000 fibers wihtin the housing, whereas this study only potted 5 fibers inside the module housing. Additionally, the most significant difference between the two dialyzers lies in the operational mode. The FX high-flux dialyzers performed a toxin removal in the IOF mode, whereas in this study the OIF mode was employed.

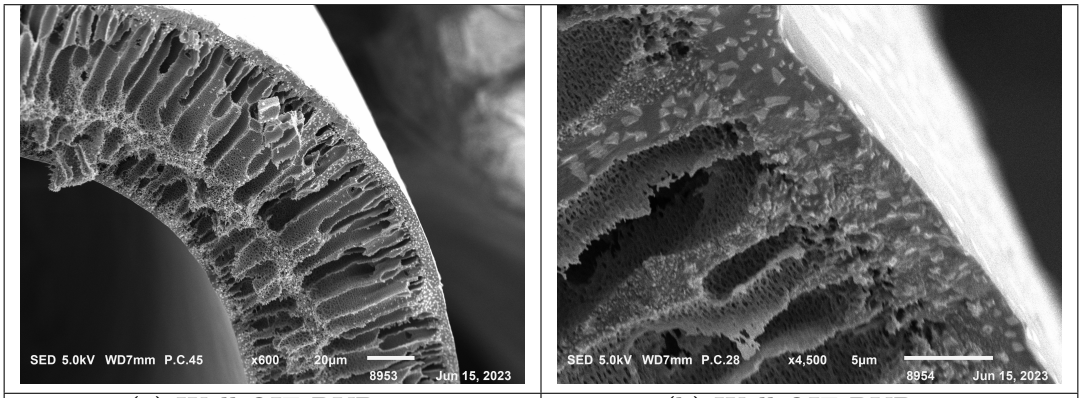

(a) Wall OIF-PVP4-3 | **(b) Wall OIF-PVP4-3**

Figure 30: SEM images of the OIF-PVP4-3 hollow fibers after performing toxin removal. The crystals observed are creatinine crystals. **(a)** Wall OIF-PVP4-3 after toxin removal (600X) **(b)** Wall OIF-PVP4-3 after toxin removal (4500X)

To check the flow of the creatinine molecules, a SEM analysis was performed of the used OIF-PVP4-3 for creatinine removal. The SEM photos are displayed in figure 30. The crystals observed are creatinine crystals. It can be clearly seen that the creatinine indeed moves through the selective inner layer and travels to the porous inner layer. It is also observed that the creatinine tends to get stuck within the sections with the smallest pores. Therefore, this explains the "creatinine removal by adsorption" of figure 28.

3.3 Hollow fiber OIF-PVP4-4

Since there was a chance that the water permeance of the OIF-PVP4-3 fibers was too low, two additional sets of fibers were made by changing the bore solution from 50/50% to a 63/37% NMP/ultrapure water solution. This formulation aimed to strike a balance between the previously used bore solutions, with the goal of achieving strong fibers with a selective outer layer and a porous inner layer. Using the initial parameters, with the bore liquid pumping speed reduced to 0.2 mL/min, the fiber failed to form correctly. Again, the fibers had difficulty not breaking and a pearl necklace was again formed. Although the fibers exhibited reduced breakage compared to those produced using the 75/25% bore solution, the desired fiber formation was not fully achieved. After discussing this fiber formation, it was hypothesized that the presence of excessive air bubbles in the bore solution could contribute to the pearl necklace appearance of the fibers.

3.4 Hollow fiber OIF-PVP4-5 & OIF-PVP4-6

To get rid of the air bubbles present in the bore solution, the bore solution was placed in the sonification bath first to degass for 30 min before the fibers were spun again. The bore solution appeared clearer and the spinning process showed notable improvement. The fibers formed successfully under the desired parameters. It was noticed that the role of the pulling wheel speed was limited due to the lack of tension. As a result, another batch of fibers was made at a pulling wheel speed of 9 m/min. This resulted in more tension in the fibers. The spinning conditions are displayed in table 8.

Table 8: Spinning conditions for the OIF-PVP4-5 and the OIF-PVP4-6 hollow fibers.

Parameters	**OIF-PVP4-5**	**OIF-PVP4-6**
Dope pumping speed ($mL\,min^{-1}$)	1.0	1.0
Bore liquid pumping speed ($mL\,min^{-1}$)	0.2	0.2
Shower pumping speed ($mL\,min^{-1}$)	0.4	0.4
Air gap (cm)	1.2	1.2
Pulling wheel speed ($m\,min^{-1}$)	4.5	9
Bore solution (NMP/MilliQ)	63/37%	63/37%
Shower solution	100% MilliQ	100% MilliQ

These two sets of fibers were analysed with the SEM and are displayed in figure 31.

(a) OIF-PVP4-5 Cross section

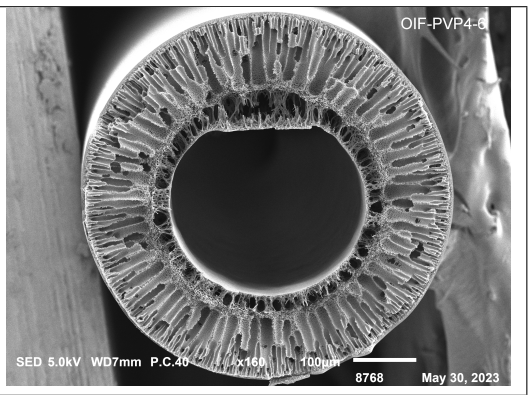

(b) OIF-PVP4-6 Cross section

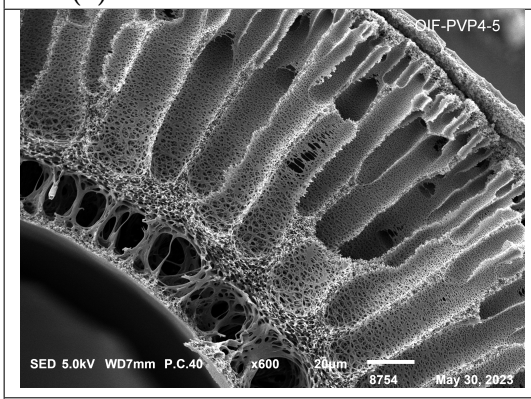

(c) OIF-PVP4-5 Wall

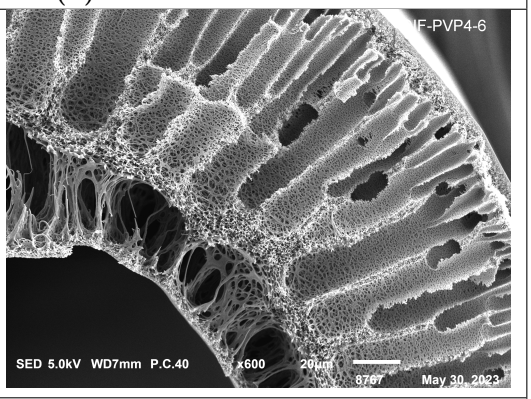

(d) OIF-PVP4-6 Wall

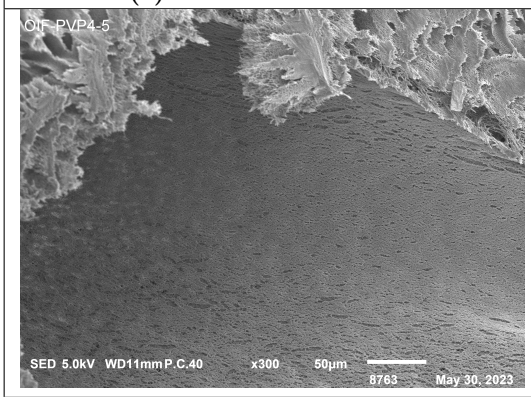

(e) OIF-PVP4-5 Inner surface

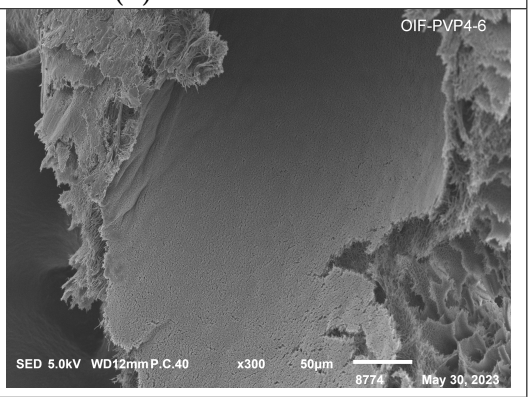

(f) OIF-PVP4-6 Inner surface

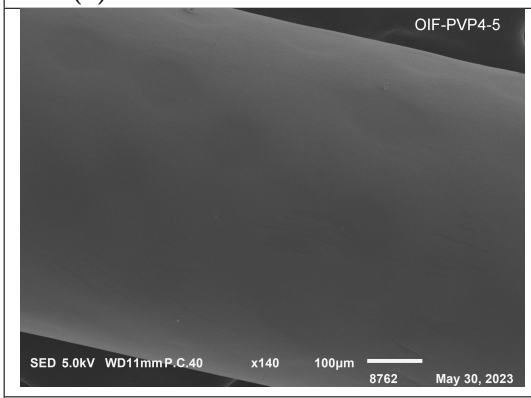

(g) OIF-PVP4-5 Outer surface

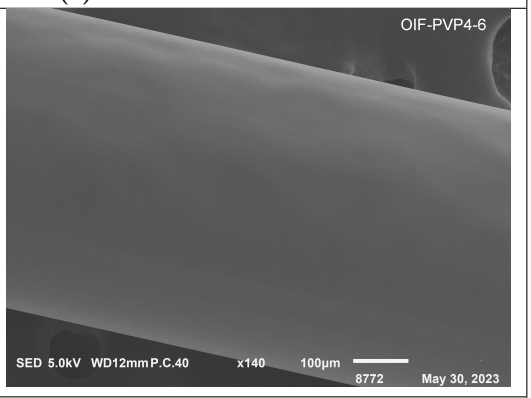

(h) OIF-PVP4-6 Outer surface

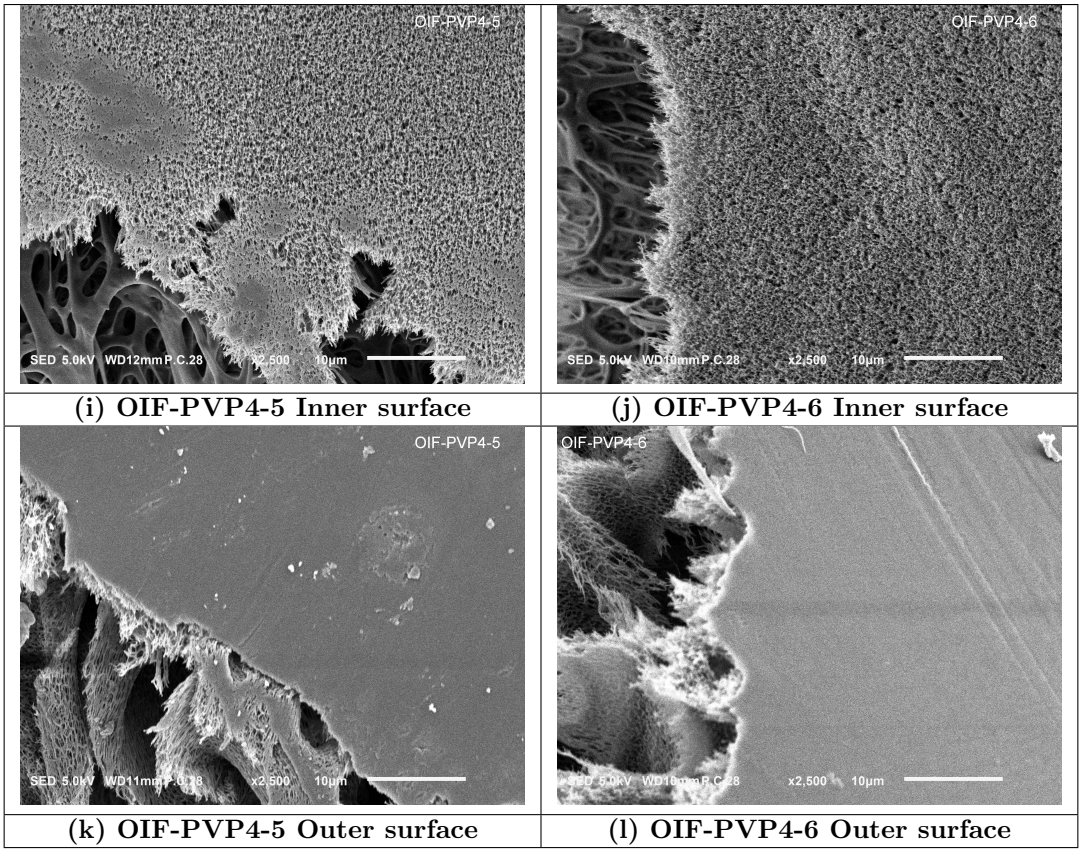

(i) OIF-PVP4-5 Inner surface | **(j) OIF-PVP4-6 Inner surface**

(k) OIF-PVP4-5 Outer surface | **(l) OIF-PVP4-6 Outer surface**

Figure 31: SEM images of OIF-PVP4-5 and OIF-PVP4-6 hollow fibers, **(a)** Cross-section OIF-PVP4-5 (140X) **(b)** Cross-section OIF-PVP4-6 (160X) **(c)** Wall OIF-PVP4-5 (600X) **(d)** Wall OIF-PVP4-6 (600X) **(e)** Inner surface OIF-PVP4-5 (300X) **(f)** Inner surface OIF-PVP4-6 (300X) **(g)** Outer surface OIF-PVP4-5 (140X) **(h)** Outer surface OIF-PVP4-6 (140X **(i)** Inner surface OIF-PVP4-5 (2500X) **(j)** Inner surface OIF-PVP4-6 (2500X) **(f)** Outer surface OIF-PVP4-5 (2500X) **(l)** Outer surface OIF-PVP4-6 (2500X)

Table 9: Measurements of the OIF-PVP4-5 and OIF-PVP4-6 hollow fibers using ImageJ.

Fiber	OIF-PVP4-5	OIF-PVP4-6
Outer diameter (µm)	662	573
Inner diameter (µm)	342	307
Wall (µm)	160	133

It can clearly be seen that the obtained fibers have a significantly thicker wall compared to the previously made OIF-PVP4 hollow fibers. Both types of fibers have a finger-like macrovoid-structured wall and a smooth, dense outer layer. However, within the inner wall of both fibers, a breakage can be observed. This breakage appears to be consistent in size across all fibers, suggesting a potential issue with the spinneret used during the spinning process. The impact of the increased pulling wheel speed is also evident in the SEM images. The fibers spun with an increased pulling wheel speed are considerable smaller compared to the fibers with the initial pulling wheel speed. This reduction in size is because of the spinning wheel stretching the fibers more when using a higher speed, resulting in thinner fibers. Furthermore, the inner layer for both fibers now have noticeable pores inside as a result of the modified bore solution. To test the effectiveness of the fibers, the water permeance and toxin removal is measured. The OIF-PVP4-6 hollow fiber is selected for this analysis due to its superior mechanical properties.

3.4.1 Water permeance OIF-PVP4-6

To measure the water permeance, the clean water flux dead-end experiment was perfomed using three modules each containing 5 fibers. The result is displayed in figure 32.

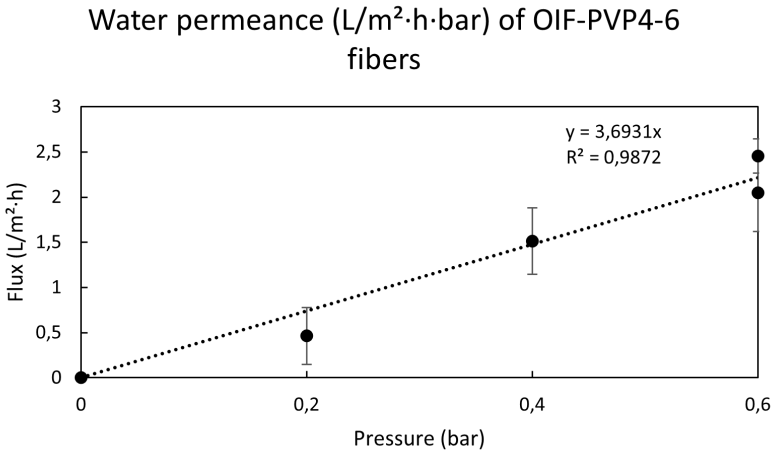

Figure 32: Water permeance measured for OIF-PVP4-6 fiber (n=3). The slope of the graph represents the water permeance ($\approx 4\ L\ m^{-2}h^{-1}bar^{-1}$).

The water permeance turned out to be really low and did not meet the desired water permeance of $\geq 20\ L\ m^{-2}h^{-1}bar^{-1}$. Interesting is that the water permeance of the OIF-PVP4-6 fiber turned out to be lower than the water permeance of the OIF-PVP4-3 fiber. It was not expected that the OIF-PVP4-6 fiber would have a lower water permeance, since the selective outer layer of both fibers looked the same based on the SEM images and were both made using a 100% ultrapure water solution as shower. To increase the water permeance, just like the OIF-PVP4-3 fibers, the fibers were treated with sodium hypochlorite.

3.4.2 Water permeance OIF-PVP4-6 after NaOCl treatment

After treating the fibers with a 4000 ppm sodium hypochlorite solution, the water permeance was measured again using the dead-end experiment. The results are displayed in figure 33.

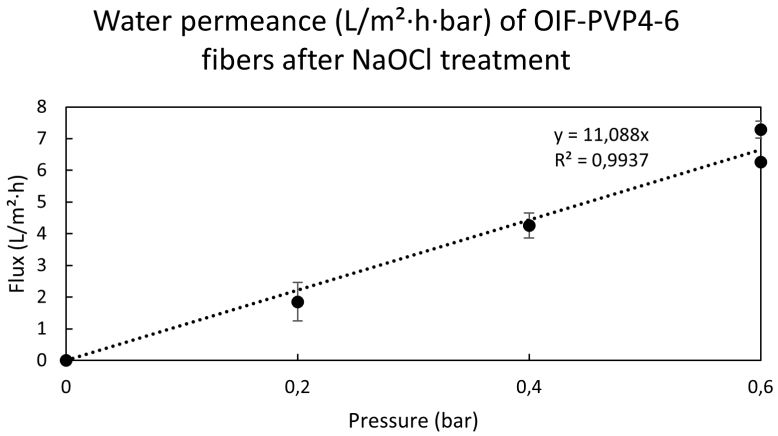

Figure 33: Water permeance measured for OIF-PVP4-6 fiber after NaOCl treatment (n=2). The slope of the graph represents the water permeance ($\approx 11\ \ L\,m^{-2}h^{-1}bar^{-1}$).

Instead of three modules, only two modules were measured correctly after sodium hypochlorite treatment, making the results less reliable. Unfortunately, the water permeance still does not meet the desired water permeance of $\geq 20\ Lm^{-2}h^{-1}bar^{-1}$, but is instead a middle-flux filter with a water permeance of approximately $11 \pm 3\,\mathrm{L\,m^{-2}}h^{-1}bar^{-1}$.

3.4.3 Toxin removal OIF-PVP4-6

For the OIF-PVP4-6 fibers, a preliminary study concerning creatinine removal was performed. Healthy human plasma was spiked with 0.1mg/mL creatinine and a cross-flow filtration in outside-in mode was performed using the Convergence set-up (n=1).The result is shown in figure 34.

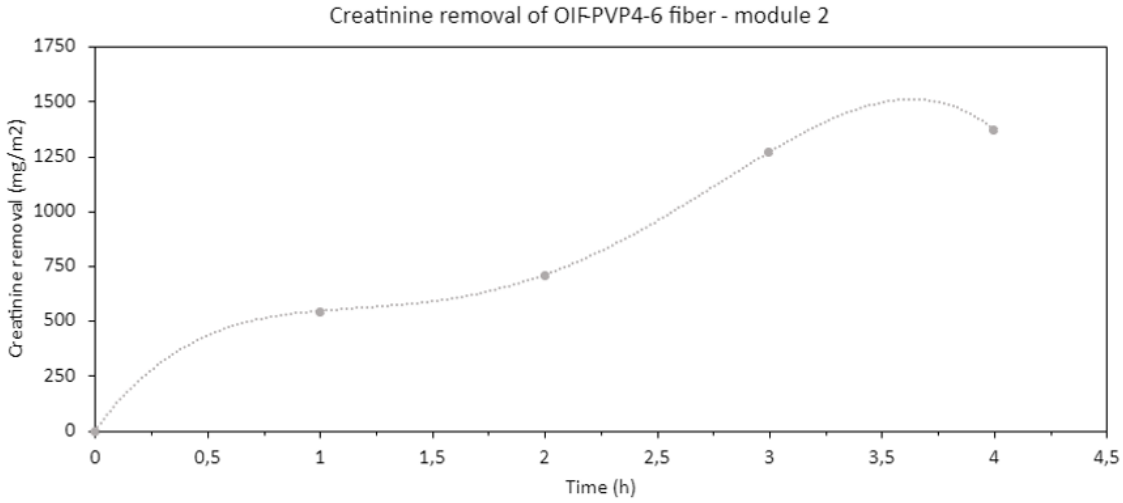

Figure 34: Creatinine removal for the OIF-PVP4-6 fiber, module 2 (n=1). The total removal is measured ($mg\,m^{-2}$).

OIF-PVP4-6 module 2 demonstrated a removal rate of 1372 $mg\,m^{-2}$ after 4h, falling out of the range of 1500 - 2000 $mg\,m^{-2}$ after 4h. Since the water permeability of the OIF-PVP4-6 fibers were lower than the water permeability of the OIF-PVP4-3 fibers, it was expected that the OIF-PVP4-6 would have a lower toxin removal. The reason for this is because creatinine is a small water-soluble toxin which can move easily through the pores, just like water. If the permeability of water turns out to be low, the permeability of creatinine is also expected to be low.

4 Conclusion

The aim of this study was to produce outside-in fibers using PVP K90 from new supplier BASF (MW $\approx$ 1000.000 Da), characterize these fibers and perform water permeability as well as toxin removal tests. This study began by testing the possibility of producing outside-in hollow fibers with a lower concentration PVP within the dope solution in order to produce fibers with the desired mechanical properties and dimensions. The PVP concentration was changed from a 5.6 wt.% to a 4 wt.% PVP concentration within the dope solution. This change was made in order to decrease the viscosity of the dope solution, making it possible to push more of the solution out of the spinneret. By pushing more out of the spinneret, the result was hypothesized to be a smaller fiber with a thicker wall. In addition, the lower PVP concentration decreases the hydrophilic properties of the dope solution, resulting in a slower movement of water present within the shower solution, bore solution and coagulation bath, creating a less sponge-like structure. After producing multiple OIF-PVP4 hollow fibers and adjusting one setting at a time, it was possible to find methods to directly change the inner layer of these fibers, as well as the size of the fibers and the structure of the fiber wall.

Influence of bore solution Decreasing the wt.% of water from 50 wt.% to 37 wt.% within the bore solution led to an enlargement of the pore size in the inner layer of the fibers due to the slowed exchange between water in the bore solution and NMP in the dope solution. Furthermore, by reducing the bore liquid pumping speed, we observed a transition from a sponge-like structured wall to a macrovoid-structured wall, resulting from diminished exchange between NMP in the dope solution and water in the bore solution.

Influence of dope solution It was hypothesized that by decreasing the wt.% PVP within the dope solution, the viscosity of the dope solution would decrease. With the viscosity being lower, more dope solution is pumped through the spinneret, resulting in smaller fibers with thicker fiber walls and thus better mechanical properties. Compared to the OIF-PVP5.6 hollow fibers, the fibers are still relatively big. The smallest fibers obtained using a 5.6 wt.% PVP had a outer diameter of 441 µm, in this study the smallest obtained fibers suited for testing were the OIF-PVP4-6 fibers, having a outer diameter of 573 µm. The fiber wall did increase in size, increasing from 40 µm for the OIF-PVP5.6 fibers to 92 µm for the OIF-PVP4-3 fibers and 133 µm for the OIF-PVP4-6 fibers. Therefore, the hypothesis is partly true and more study is necessary in order to decrease the fiber size. In addition, it was hypothesized that the decreased wt.% PVP would result in a "slower water movement" present within the shower solution, bore solution and coagulation bath. The slower movement was thought to result in a less sponge-like structured wall, which is indeed the case in this study. All the fibers produced during this study consisted of a macrovoid-structured wall, proving that the hypothesis is indeed correct.

Influence of pulling wheel speed The size of the fibers decreased as the pulling wheel speed increased, intensifying the tension exerted during fiber fabrication, resulting in smaller fibers.

Water permeance The fibers with the best mechanical properties and structure, OIF-PVP4-3 and OIF-PVP4-6 hollow fibers, were further analyzed by measuring the water permeance and the creatinine removal. The OIF-PVP4-3 hollow fibers gave the desired minimal value for the water permeance, having a water permeance of $\geq 20\ L\,m^{-2}h^{-1}bar^{-1}$ after NaOCl treatment. The OIF-PVP4-6 hollow fibers had a water permeance of approximately 11 $L\,m^{-2}h^{-1}bar^{-1}$ after NaOCl treatment, which is too low to be a high-flux membrane. It is preferred to obtain a high-flux water permeance without bleaching. Therefore, further study is necessary in order to increase the water permeance without bleaching.

Toxin removal The OIF-PVP4-3 hollow fibers had a creatinine removal of 1630 $\pm$ 171 $mg\,m^{-2}$ after 4h, which does fall within the creatinine removal range of 1500 - 2000 $mg\,m^{-2}$ after 4h. This range was preferred since the OIF-PVP5.6 hollow fibers made with PVP K90 from Sigma-Aldrich had this range for creatinine removal. The dialysance found was 395 $mL\,m^{-2}\,min^{-1}$ for the OIF-PVP4-3 hollow fibers. This dialysance is higher than the clearance of the FX high-flux dialyzers, which ranged from 138 to 240 $mL\,m^{-2}\,min^{-1}$. However, it needs to be taken into consideration that there were multiple different conditions used for both toxin removal measurements, such as the mode used (OIF

vs IOF), differences in using plasma or blood and different flow rates for both the blood/plasma and dialysis solution.

As expected, the creatinine removal for the OIF-PVP4-6 hollow fibers were lower than for the OIF-PVP4-3 hollow fibers, as a result of a lower water permeability. The creatinine removal of OIF-PVP4-6 module 2 was 1372 $mg\,m^{-2}$ after 4h. Because only one module of the OIF-PVP4-6 was tested, more research is necessary in order to have reliable results for the OIF-PVP4-6 fibers.

Ultimately, the primary goal of this research is to contribute to the development of hollow fibers that possess the desired dimensions, high-flux characteristics, and exceptional toxin removal capabilities for outside-in dialysis therapy. Although the fibers produced in this study did not meet these specific requirements, the insights gained regarding the manipulation of mechanical properties and structure are crucial steps in the right direction. By advancing our understanding and refining the fabrication techniques, we strive to enhance the overall quality of life for individuals suffering from kidney diseases. Improving the efficacy and performance of dialysis membranes directly translates into improved patient outcomes and a better standard of living for kidney patients.

5 Outlook

Obtaining preferred dimensions To further optimize the dimensions of the hollow fibers and enhance the efficiency of the dialyzer, additional research can focus on achieving smaller fibers with specific outer diameter and wall thickness. The desired dimensions include an outer diameter of approximately 350 µm and a wall thickness of around 40 µm. By reducing the fiber size, a larger number of fibers can be accommodated within the modules, utilizing a more efficient dialyzer. Both the OIF-PVP5.6 and OIF-PVP4 hollow fibers indicate that increasing the pulling wheel speed results in smaller fiber dimensions. Another parameter that holds the potential to influence fiber thickness and the overall fiber diameter is the dope pumping speed. Decreasing the dope pumping speed will lead to a decrease in the overall fiber diameter. When the dope pumping speed is increased and the pulling wheel speed is increased as well, the result could be a smaller fiber with a thicker wall. Therefore, it is recommended to explore and manipulate these parameters to obtain the desired smaller fiber size with the preferred wall thickness. Investigating the impact of varying dope pumping speeds and pulling wheel speeds on fiber dimensions will provide valuable insights into optimizing the fabrication process and achieving the desired fiber dimensions.

Further research OIF-PVP4-3 It is adviced to focus on further development of the OIF-PVP4-3 hollow fibers, as these fibers have demonstrated the best permeability and toxin removal performance. Additionally, the aspect ratio between wall thickness and outer diameter is reasonably aligned with the desired dimensions. However, it is necessary to test whether these membranes are capable of filtering larger toxins, such as protein-bound toxins (hippuric acid (HA) and indoxyl sulfate (IS)) and middle molecules (β_2-microglobulin). This can be investigated using HPLC analysis. It would also be interesting to perform the toxin removal in the IOF modus for comparison to the OIF modus, to prove that the OIF modus indeed has a better toxin removal.

Increase permeability Furthermore, it is crucial to explore methods for enhancing the permeability of the fibers, eliminating the need for bleaching. Increasing the pore size can be achieved by modifying the shower solution. Introducing a small percentage of NMP to the shower solution will slow down the exchange between water from the shower and NMP from the dope solution, resulting in slightly larger pores. A starting point could be a water/NMP ratio of 95/5%.

OIF modus clean water flux In addition to the permeability of the fibers, it is interesting to look at measuring the water permeability in the OIF modus instead of the IOF modus. In the OIF mode, the permeability of the fiber results in water being forced into the fiber, rather than water being pushed outwards from the fiber. While it is expected that this does not affect the measured permeability of the fiber, it could possibly impact the mechanical forces exerted on the fiber. Normally, internal pressure is applied to the fiber, whereas in the OIF mode, pressure is applied in the opposite direction, from the outside towards the fiber. Exploring the potential influence of this change in pressure on fiber properties such as fracture behavior and structural integrity is of great interest. It is intriguing to investigate whether this altered pressure condition could affect the fiber's strength and stability. In order to do this, the clean water flux set-up can be used. Instead of pushing the water through the fibers to enter the module, the water enters the module through one of the T-connectors, while the other T-connector is closed off. One end of the module is closed off, while the other end is now open. Because of the applied pressure, the water is now pushed from the outside to the inside of the fiber and leaves the module through the open fiber end of the module. In order to prevent collapsing of the fibers because of the sudden pressure change, it is advised to fill the module either with more fibers or to fill up the module with water by hand first.

Conditions toxin removal To facilitate a more accurate comparison of toxin removal, it is recommended to perform toxin removal tests on the OIF-PVP4-3 fibers under conditions similar to those employed for the commercial FX high-flux dialyzers, with the exception of the mode of operation. Adjusting the flow rate of the OIF-PVP4-3 fibers to a comparable ratio between blood and dialysis solution utilized by the commercial fibers would be beneficial. Furthermore, exploring toxin removal using blood instead of plasma could provide valuable insights into the toxin removal capabilities of the OIF-PVP4-3 fibers in relation to the FX high-flux dialyzers. This approach will contribute to a

better understanding of the performance of the OIF-PVP4-3 fibers in comparison to the commercial FX high-flux dialyzers.

Further research OIF-PVP4-6 As mentioned in the results, further research regarding the OIF-PVP4-6 hollow fibers is necessary to provide a understanding of these outcomes and to obtain reliable results. The first step would be replicating the spinning process for the OIF-PVP4-6 fibers, using the same parameters and solutions. However, it is crucial to ensure that the spinneret remains unobstructed. Then, the same tests as done previously need to be performed for more modules, a minimum of 3 recommended, in order to obtain reliable results for the toxin removal of these fibers and to check if the breakage of the inner wall did or did not have an influence on the results obtained in this study. Having reliable results for the OIF-PVP4-6 hollow fibers would give more insight in the influence of the bore solution, when compared to the OIF-PVP4-3 hollow fibers.

Bovine serum albumin (BSA) test Conducting a bovine serum albumin (BSA) test would be of great interest to assess membrane fouling. This test can be performed utilizing the clean water flux set-up and analyzing with the nanodrop. To execute the BSA test, BSA is dissolved in a PBS solution and passed through the fibers in the OIF mode. Similar to permeability measurements, one end of the module is closed (dead-end experiment), and the solution drips through the open end into a collection container. Subsequently, the collected solution is analyzed using the nanodrop to quantify the amount of BSA retained within the fibers versus the amount that diffused through the fiber and was collected in the container. To pinpoint the specific locations where BSA becomes entrapped within the fiber membrane, a fluorescent label can be incorporated into the BSA and examined using a confocal microscope. This approach enables a understanding of the filtration behavior and facilitates identification of potential fouling areas within the fiber structure.

6 Acknowledgement

I would like to express my gratitude for the tremendous support I have received during the past 10 weeks, despite the busy schedules of those around me. First and foremost, I would like to thank David Ramada for his guidance in the laboratory, his valuable insights into the research, and his willingness to assist whenever needed. It has been a pleasure to contribute to your research, and I wish you continued success in your research. I would also like to extend my heartfelt thanks to my dear partner Arend and my parents for their mental support throughout these 10 weeks. Furthermore, I would like to thank Iris Allijn and Dimitrios Stamitialis for their critical questions and their valuable input into the research. Their thought-provoking inquiries have provided me with new perspectives and greatly influenced the progress of my work. Lastly, I want to express my deepest gratitude to Odyl ter Beek. Odyl has been instrumental in my journey over the past 10 weeks, constantly offering insights, providing explanations whenever needed, engaging in discussions about the results, and guiding me in determining the next steps. Moreover, Odyl has been an incredible source of support throughout the process, always available for questions and assistance. Thank you so much.

References

[1] C. P. Kovesdy, "Epidemiology of chronic kidney disease: an update 2022," *Kidney international supplements*, vol. 12, no. 1, pp. 7–11, 4 2022. [Online]. Available: https://pubmed.ncbi.nlm.nih.gov/35529086/

[2] "Your Kidneys & How They Work - NIDDK." [Online]. Available: https://www.niddk.nih.gov/health-information/kidney-disease/kidneys-how-they-work

[3] L. E. Thompson and M. S. Joy, "Endogenous markers of kidney function and renal drug clearance processes of filtration, secretion, and reabsorption," *Current Opinion in Toxicology*, vol. 31, p. 100344, 9 2022.

[4] M. S. McManus and S. Wynter-Minott, "Guidelines for Chronic Kidney Disease: Defining, Staging, and Managing in Primary Care," *The Journal for Nurse Practitioners*, vol. 13, no. 6, pp. 400–410, 6 2017.

[5] "CKD Stages — The UK Kidney Association." [Online]. Available: https://ukkidney.org/health-professionals/information-resources/uk-eckd-guide/ckd-stages

[6] S. Vadakedath and V. Kandi, "Dialysis: A Review of the Mechanisms Underlying Complications in the Management of Chronic Renal Failure," *Cureus*, vol. 9, no. 8, 8 2017. [Online]. Available: /pmc/articles/PMC5654453//pmc/articles/PMC5654453/?report=abstracthttps://www.ncbi.nlm.nih.gov/pmc/articles/PMC5654453/

[7] "Peritoneal Dialysis - NephCure." [Online]. Available: https://nephcure.org/peritoneal-dialysis/

[8] "BLOOD CIRCUIT FOR HEMODIALYSIS by Dr. Jigar Shrimali – Glom India." [Online]. Available: https://glomindia.com/blood-circuit-for-hemodialysis-drjigarshrimali/

[9] B. Krause, M. Storr, T. Ertl, R. Buck, H. Hildwein, R. Deppisch, and H. Göhl, "Polymeric Membranes for Medical Applications," *Chemie-Ingenieur-Technik*, vol. 75, no. 11, pp. 1725–1732, 2003. [Online]. Available: https://www.researchgate.net/publication/229795056_Polymeric_Membranes_for_Medical_Applications

[10] "Progress in Hemodialysis: From Emergent Biotechnology to Clinical Practice - Google Books." [Online]. Available: https://books.google.nl/books?hl=en&lr=&id=vnSfDwAAQBAJ&oi=fnd&pg=PA65&dq=Polyethersulfone+Hollow+Fiber+Membranes+for+Hemodialysis&ots=Z9yKm_K4xt&sig=zUeNhcRYK-dwSHwyXPCESDNKFfs#v=onepage&q=Polyethersulfone%20Hollow%20Fiber%20Membranes%20for%20Hemodialysis&f=false

[11] S. S. Dukhin, Y. Tabani, R. Lai, O. A. Labib, A. L. Zydney, and M. E. Labib, "Outside-in hemofiltration for prolonged operation without clogging," *Journal of Membrane Science*, vol. 464, pp. 173–178, 8 2014.

[12] O. E. ter Beek, D. Pavlenko, and D. Stamatialis, "Hollow fiber membranes for long-term hemodialysis based on polyethersulfone-SlipSkin™ polymer blends," *Journal of Membrane Science*, vol. 604, p. 118068, 6 2020.

[13] O. E. ter Beek, M. K. van Gelder, C. Lokhorst, D. H. Hazenbrink, B. H. Lentferink, K. G. Gerritsen, and D. Stamatialis, "In vitro study of dual layer mixed matrix hollow fiber membranes for outside-in filtration of human blood plasma," *Acta Biomaterialia*, vol. 123, pp. 244–253, 3 2021.

[14] I. Geremia, "New membrane strategies for improved artificial kidney devices," 1 2021. [Online]. Available: https://research.utwente.nl/en/publications/new-membrane-strategies-for-improved-artificial-kidney-devices

[15] "FX high and low-flux dialyzers — Fresenius Medical Care." [Online]. Available: https://www.freseniusmedicalcare.com/en/healthcare-professionals/hemodialysis/dialyzers/fx-high-and-low-flux-dialyzers

[16] B. J. Inkson, "Scanning electron microscopy (SEM) and transmission electron microscopy (TEM) for materials characterization," *Materials Characterization Using Nondestructive Evaluation (NDE) Methods*, pp. 17–43, 1 2016.

[17] D. L. Kim and D. Stamatialis, "High flux mixed matrix membrane with low albumin leakage for blood plasma detoxification," *Journal of Membrane Science*, vol. 609, p. 118187, 8 2020.

[18] G. Dibrov, G. Kagramanov, V. Sudin, E. Grushevenko, A. Yushkin, and A. Volkov, "Influence of Sodium Hypochlorite Treatment on Pore Size Distribution of Polysulfone/Polyvinylpyrrolidone Membranes," *Membranes 2020, Vol. 10, Page 356*, vol. 10, no. 11, p. 356, 11 2020. [Online]. Available: https://www.mdpi.com/2077-0375/10/11/356/htmhttps://www.mdpi.com/2077-0375/10/11/356

[19] J. Chokki, G. Darracq, P. Poelt, J. Baron, H. Gallard, M. Joyeux, and B. Teychené, "Investigation of Poly(ethersulfone)/Polyvinylpyrrolidone ultrafiltration membrane degradation by contact with sodium hypochlorite through FTIR mapping and two-dimensional correlation spectroscopy," *Polymer Degradation and Stability*, vol. 161, pp. 131–138, 3 2019.